Food and Chemical Toxicology 197 (2025) 115241

Contents lists available at ScienceDirect

Food and Chemical Toxicology

journal homepage: www.elsevier.com/locate/foodchemtox

Impact of endocrine disruptors on key events of hepatic steatosis in HepG2 cells

Marina F. Grosso, Eliška Řehůřková, Ishita Virmani, Eliška Sychrová, Iva Sovadinová, Pavel Babica *

RECETOX, Faculty of Science, Masaryk University, Kotlářská 2, 61137, Brno, Czech Republic

A R T I C L E I N F O

Handling Editor: Dr. Bryan Delaney

Keywords:
High-content imaging
In vitro testing
Lipid droplets
Metabolism-disrupting chemicals
NAFLD
NAMs

A B S T R A C T

Endocrine-disrupting chemicals (EDCs) may contribute to the rising incidence of metabolic dysfunction-associated steatotic liver disease (MASLD). We investigated the potential of 10 environmentally relevant EDCs to affect key events of hepatic steatosis in HepG2 human hepatoblastoma cells. Increased lipid droplet formation, a key marker of steatosis, was induced by PFOA, bisphenol F, DDE, butylparaben, and DEHP, within the non-cytotoxic concentration range of 1 nM–25 μM. Cadmium also induced this effect, but at concentrations impairing cell viability (>1 μM). At non-cytotoxic concentrations, these compounds, along with bisphenol A, dysregulated major genes controlling lipid homeostasis. Cadmium, PFOA, DDE, and DEHP significantly upregulated the *DGAT1* gene involved in triglyceride synthesis, while butylparaben increased the expression of the *FAT/CD36* gene responsible for fatty acid uptake. Bisphenol A downregulated the *CPT1A* gene involved in fatty acid oxidation. No significant effects on lipid droplet accumulation or lipid metabolism-related genes were observed for PFOS, bisphenol S, and dibutyl phthalate. Among the tested EDCs, lipid accumulation positively correlated with the expression of *SREBF1*, *DGAT1*, and *CPT1A*. These findings provide additional evidence that EDCs can affect MASLD and highlight the utility of *in vitro* methods in the screening of EDCs with hazardous steatogenic and metabolism-disrupting properties.

1. Introduction

Metabolic disorders, such as obesity, type 2 diabetes, or chronic liver metabolic diseases, are becoming increasingly prevalent worldwide. This rise can be attributed to a combination of genetic background and lifestyle changes, including diet, exercise, therapeutic drug use, and aging. However, there is mounting evidence that exposure to environmental toxicants can influence the onset and development of these metabolic disorders (Heindel et al., 2017, 2022).

Among environmental toxicants, endocrine disrupting chemicals (EDCs) represent a heterogeneous group of substances (Cano et al., 2021), including industrial chemicals (e.g., dioxins, polychlorinated biphenyls, alkylphenols), agricultural (e.g., insecticides, herbicides, fungicides), residential (e.g., phthalates, polybrominated biphenyls, bisphenols), pharmaceutical and personal care products (e.g., parabens), some heavy metals (e.g., cadmium), or natural compounds (e.g., phytoestrogens). EDCs interfere with physiological hormonal signaling via various mechanisms, causing hormonal dysregulations and consequently increasing the risk of several pathologies, including metabolic disorders (Cano et al., 2021; Heindel et al., 2022; Mosca et al., 2024). Several EDCs have been recognized to impact metabolic functions and act as metabolism-disrupting chemicals (MDCs). The liver, being the central organ of metabolism in a body, is one of the main targets of MDCs. Metabolic dysfunction-associated fatty liver disease (MASLD), formerly known as non-alcoholic fatty liver disease (NAFLD), represents a prevalent chronic metabolic liver disease affecting up to 25% of the global population (Cano et al., 2021; Rinella et al., 2023). MASLD covers a broad spectrum of liver conditions occurring in individuals without significant alcohol consumption but with at least one metabolic risk factor. These conditions range from simple metabolic dysfunction-associated steatotic liver (MASL), also known as hepatic steatosis, characterized by an excessive fat build-up in more than 5% of hepatocytes, to metabolic dysfunction-associated steatohepatitis (MASH), which is characterized by liver tissue injury, inflammation, and fibrosis. MASLD can sensitize the liver to cirrhosis and hepatocellular carcinoma (Cano et al., 2021; Heindel et al., 2022; Mosca et al., 2024).

* Corresponding author.
E-mail address: pavel.babica@recetox.muni.cz (P. Babica).

https://doi.org/10.1016/j.fct.2025.115241
Received 3 September 2024; Received in revised form 2 December 2024; Accepted 5 January 2025
Available online 6 January 2025

Based on current mechanistic understanding encapsulated by adverse outcome pathways (AOP) for hepatic steatosis, chemicals inducing MASLD can interact with nuclear receptors (e.g., PPARα/γ, LXR, PXR, AhR, CAR, RAR, FXR, or GR), representing a molecular initiating event, i.e. MIE (Angrish et al., 2016; Escher et al., 2022; Kubickova and Jacobs, 2023; Lichtenstein et al., 2020). Dysregulation of these receptors alters the expression of genes controlling intracellular lipid homeostasis through the four key events (KEs): 1) hepatocellular uptake of circulating lipids; 2) *de novo* lipogenesis (e.g., fatty acid synthesis and triglyceride synthesis), 3) mitochondrial and peroxisomal fatty acid oxidation; and 4) hepatocellular lipid efflux. Dysregulation of these processes leads to an imbalance between lipid acquisition and disposal, resulting in the accumulation of triglycerides in cytoplasmic lipid droplets. Excessive accumulation of fatty acids and droplets can then cause cytoplasmic displacement, nuclear distortion, mitochondrial dysfunction, and endoplasmic reticulum stress. The more severe MASH condition is associated with lipotoxicity, oxidative stress, inflammation, and cell death (Angrish et al., 2016; Escher et al., 2022; Kubickova and Jacobs, 2023; Lichtenstein et al., 2020). These mechanisms have been relatively well-studied in response to certain therapeutic drugs with pro-lipogenic or steatogenic effects, such as amiodarone, valproic acid, tetracycline, or cyclosporin A (Donato et al., 2022; Escher et al., 2022; Kubickova and Jacobs, 2023).

Although considerable epidemiological, computational, and experimental evidence links certain EDCs to MASLD, the underlying mechanisms by which various compounds disrupt lipid metabolism and cause steatosis are not fully understood. Mechanistic understanding of steatosis-related effects in human liver cells is primarily available for a few prominent EDCs (Fritsche et al., 2023; Kowalczyk et al., 2023; Kubickova and Jacobs, 2023). However, even for these compounds, the available data are often scattered across multiple studies that used different experimental designs, conditions, endpoints, and methods. Moreover, there are about 1000 chemicals currently recognized as EDCs, but for most of them, data on their metabolic-disrupting activities are missing (Heindel et al., 2022; Mosca et al., 2024). Furthermore, recognized EDCs represent only a fraction of the chemicals released into the environment due to human activities that have not yet been evaluated for their metabolic-disrupting effects. This gap is partly due to the current lack of validated tests specifically designed to assess the hazards and risks associated with metabolic disruption, including MASLD (Kubickova and Jacobs, 2023). Further research is thus needed to investigate the steatogenic effects of EDCs or other chemicals and to develop and validate suitable test methods for the assessment of hepatic steatosis and MASLD (Audouze et al., 2020; Kubickova and Jacobs, 2023; Küblbeck et al., 2020; Legler et al., 2020). The development of animal-free, human-relevant *in silico* and *in vitro* tools, collectively known as new approach methodologies (NAMs), is currently prioritized for integration into frameworks such as integrated approaches for testing and assessment (IATA) to support regulatory decision-making (Audouze et al., 2020; Kubickova and Jacobs, 2023).

Therefore, our work aimed to expand the existing knowledge on the steatogenic effects of EDCs by investigating the impact of 10 selected compounds: cadmium, p,p'-dichlorodiphenyldichloroethylene (DDE), perfluorooctanoic acid (PFOA), perfluorosulfonic acid (PFOS), butylparaben, bisphenol A (BPA), bisphenol S (BPS), bisphenol F (BPF), bis (2-ethylhexyl) phthalate (DEHP) and dibutyl phthalate (DBP). These chemicals were selected to represent major groups of EDCs with respect to their widespread environmental presence, human exposure, supporting epidemiological and toxicological data on their metabolism-disrupting activity, and regulatory interests (Audouze et al., 2020; Cano et al., 2021; Fritsche et al., 2023; Mosca et al., 2024). The steatogenic effects were studied *in vitro* using the human liver cell line HepG2, previously successfully utilized to study lipid accumulation and steatosis-relevant processes in response to selected EDCs (Lin et al., 2017; Liu et al., 2020; Negi et al., 2021; Peyre et al., 2014; Wen et al., 2020). We aimed to investigate the effects of a set of EDCs whose metabolic-disrupting activities were recently explored across experimental concentrations ranging from 10 pM to 25 μM in different experimental models, including pancreatic cells (Al-Abdulla et al., 2022, 2023), adipose tissue cells (Kucera et al., 2024), hepatic cells (Bernal et al., 2024), and a zebrafish steatogenic assay (Le Mentec et al., 2023). In our study, we evaluated their effects on HepG2 cellular viability, cell growth, lipid accumulation, and alterations of selected gene markers controlling lipid homeostasis using a 96-well microplate format facilitated by automated imaging and image analysis. This approach offered an easy-to-use protocol that provided insights into the steatogenic potential and mechanisms of EDCs and could be utilized in the screening of MDCs.

2. Materials and methods

Chemicals. All ingredients for phosphate-buffered saline (PBS, pH 7.2), ethanol, acetic acid, paraformaldehyde, dimethyl sulfoxide (DMSO), Neutral Red, Thiazolyl Blue Tetrazolium Bromide (MTT) and DAPI were purchased from Sigma-Aldrich (Prague, Czech Republic). AlamarBlue, CFDA-AM (5-carboxyfluorescein diacetate, acetoxymethyl ester), and Bodipy 493/503 were purchased from Thermo Fisher Scientific (Waltham, MA). The studied chemical compounds were obtained from Sigma-Aldrich: BPA (#239658), BPS (#103039), BPF (#B47006), DEHP (#36735), DBP (#524980), PFOA (#171468), PFOS (#77282), $CdCl_2$ (#202908), DDE (#35487), butylparaben (#54680), amiodarone (#A8423), palmitic acid (#P5585), oleic acid (#O1008), L-ascorbic acid 2-phosphate (#A8960), anthracene (#141062), caffeine (#C0750), D-mannitol (#M4125), caproclactam (#C2204), sodium citrate (#PHR1416), chloroquine (CQ, #C6628), tributyltin chloride (TBT, #T50202), etoposide (#E1383), triclosan (TCS, #72779), diisononyl cyclohexane-1,2-dicarboxylate (DINCH, #Y0002022), and rosiglitazone (RGZ, #R2408). Tris(methylphenyl) phosphate (TMPP, #P0273) was purchased from the Tokyo Chemical Industry Europe (Paris, France). The chemical compounds were diluted in DMSO to prepare 1000 × stock solutions, except ascorbic acid, citrate, and caffeine, which were dissolved in sterile ultrapure Milli-Q water.

Cell cultivation. The human hepatoblastoma (Arzumanian et al., 2021) cell line HepG2 (ATCC HB-8065) was obtained from LGC Standards (Łomianki, Poland). The cells were grown in low glucose (1 g/L) Minimum Essential Medium (MEM, Gibco #61100, Thermo Fisher), supplemented with 1% (v/v) MEM Non-Essential Amino Acids (Gibco #111400, Thermo Fisher), 1 mM sodium pyruvate (Thermo Fisher), and sodium bicarbonate (1.5 g/L, Sigma-Aldrich). The medium was supplemented with 10% (v/v) fetal bovine serum (#1001/500, Biosera, Nuaillé, France) and sterile-filtered (0.2 μm PES filter, TPP, Trasadingen, Switzerland). The cells were routinely cultured as monolayer cultures in 25 cm^2 cell culture flasks (TPP) and passaged twice per week before reaching 80% confluency. The cells were detached using trypsin/EDTA (Thermo Fisher), re-suspended, and diluted three-fold with fresh culture medium before being transferred to a new flask for further propagation. The cells between passages 15–30 were used for the experiments. The lack of mycoplasma contamination was regularly checked using the Mycoplasmacheck Service (Eurofins Genomics, Ebersberg, Germany). The cells were seeded at 40,000 cells/cm^2 (100 μL cell suspension/well) for all experiments in 96-well microplates. The cells were seeded into the inner 60 wells of the plate with the peripheral wells filled with 200 μL PBS to minimize the effects of evaporation, except for impedimetric experiments, where the entire plate was used and placed in the xCELLigence monitoring module. The cells were cultured for 24 h prior to the chemical exposures. All cultivations and exposures were conducted in an incubator at 37 °C with a 5% CO_2 humidified atmosphere.

Chemical exposure. The stock solutions were diluted 500-fold in a complete cell culture medium to achieve 2 × of the desired exposure concentration. Then, 100 μL of the 2 × exposure solution was added to cells cultured in 100 μL in 96-well microplates, resulting in a final 1000-fold dilution. The vehicle concentration did not exceed 0.1% (v/v) of

DMSO or sterile water, respectively. Non-treated and solvent-treated cells were included and evaluated as negative controls in each experiment. The cells were exposed for 48 h, except for impedimetric Real-Time Cell Analysis (RTCA) using the xCELLigence system, which ran for 144 h.

Cytotoxicity assays. Cell viability was evaluated using a combination of three indicator dyes: resazurin (for dehydrogenase activity assessment), CFDA-AM (for esterase activity and membrane integrity assessment), and Neutral Red uptake (NRU, for the uptake and lysosomal retention of Neutral Red dye) as reported previously (Raška et al., 2018). In parallel, cell viability was also evaluated using the MTT assay. The assays were conducted in black 96-well microplates with transparent bottoms (Greiner Bio-One, Kremsmunster, Austria), with chemical and control treatments conducted in triplicates. After 48-h exposure, the cells were rinsed with PBS and incubated in serum-free MEM medium (Gibco #51200, Thermo Fisher) containing 5% v/v AlamarBlue (ready-to-use resazurin solution) and 4 μM CFDA-AM. After a 30-min incubation, the fluorescence was measured using BioTek Synergy 4 Reader (Agilent, Winooski, VT) at 485/520 nm (CFDA-AM) and 530/590 nm (resorufin) excitation/emission. The dye solution was then aspirated, and the cells were rinsed with PBS and incubated for 2 h with 50 μg/mL Neutral Red dissolved in serum-free culture media. After rinsing with PBS, accumulated Neutral Red was extracted with 50% (v/v) ethanol-1% (v/v) acetic acid and quantified spectrophotometrically using Biotek Synergy Mx (Agilent) at 540 nm with 690 nm reference wavelength. For the MTT assay, the treated cells were rinsed with PBS and incubated for 2 h with 500 μg/mL MTT dissolved in the serum-free MEM medium. The medium was carefully aspirated, and MTT formazan was solubilized and extracted from the cells using 100 μL DMSO. Absorbance was measured at 570 nm with 690 nm reference wavelength using Biotek Synergy Mx (Agilent). Fluorescence and absorbance readings from the assay blank wells without cells were subtracted from the experimental wells before data analysis. Blank-subtracted values were compared to the average of the non-treated control wells and expressed as a fraction of the control (FOC).

Real-Time Cell Analysis (RTCA). Continuous and real-time impedimetric measurements were conducted using the xCELLigence RTCA SP Instrument (ACEA Biosciences, San Diego, CA). For RTCA experiments, HepG2 cells were seeded in a 96-well E-Plate VIEW 96 microplate (ACEA Biosciences). Cell impedance was monitored every minute for the first 4 h and every hour for the next 24 h. After this period, the cells were treated with selected chemicals and controls, with each treatment conducted in quadruplicate. During exposure, cell index (CI) values were recorded every 15 min for the first 3 h and every hour for the next 144 h (6 days). The relative change in electrical impedance caused by adherent cells was expressed as CI values, that are directly proportional to changes in cell number, size, morphology, adhesion, proliferation, or cell-cell interactions. These CI values were recalculated to Normalized Cell Index (NCI) values, representing CI readouts from each well normalized to the cell impedance at the beginning of the exposure, i.e., 24 h after the cell seeding. The NCI values in the treated wells were compared to the averaged NCI in the non-treated control wells at a given time point and expressed as FOC. After 144-h exposure, the NRU assay was also conducted as described above.

Lipid accumulation assay. The HepG2 cells were seeded in a 96-well black plate with a transparent bottom (Greiner Bio-One) for 24 h and then treated for 48 h with selected chemicals and controls. Positive controls included cells treated with 200 μM of palmitic:oleic acid (PAOA) mixture (1:2), 10 μM amiodarone, and/or 10 μM TMPP, which induced lipid accumulation under our experimental conditions. Each treatment was conducted in triplicate. After exposure, the cell culture media was discarded, and cells were rinsed with PBS and fixed for 20 min in 4% (w/v) paraformaldehyde to preserve lipid droplet structures. Then, the cells were rinsed with PBS, and lipid droplets were stained for 30 min with 1.25 μg/mL of Bodipy 493/503 (in PBS), while keeping the plate in the dark. The cells were then rinsed again with PBS and counterstained for 10 min with 1.25 μg/mL DAPI solution in PBS. Microscopic images were acquired using Biotek Cytation 5 Cell Imaging Multi-Mode Reader (Agilent) with 20 × objective, using GFP and DAPI filter cubes for lipid droplets and nuclei staining, respectively. A montage of 3 × 3 fields of view was taken from each well using both fluorescence channels, covering a 0.75 mm^2 growth area (1032 μm × 723 μm). With a cell density of approximately 220,000 cells/cm^2 in the non-treated or solvent control, this setup allowed the evaluation of ~1650 individual cells per well, i.e., about ~5000 cells combined per triplicate treatment. This protocol enables the evaluation and quantitative analysis of lipid accumulation (cell counts, area/mean intensity/integrated intensity of lipid droplets per cell) in a 96-well plate within 90 min.

Acquired images were analyzed using BioTek Gen5 software (Agilent) to segment lipid droplets (GFP channel) and nuclei (DAPI channel). Integrated (total) fluorescence intensity of lipid droplets (i.e., droplet area × mean fluorescence intensity) was used as an integrative parameter reflecting droplet size, number, and intensity. The integrated fluorescence intensity of the droplets was then divided by the cell (nuclei) count in the given image. The cell count-normalized values obtained for each image were then compared to the average value obtained for the non-treated control wells from a given microplate and expressed as FOC. Nuclei count in each image was compared to the average nuclei count in the non-treated control wells and expressed as FOC to reflect the effects of chemicals on cell density due to eventual inhibition of proliferation and cytotoxicity.

Quantitative reverse transcription PCR (RT-qPCR). HepG2 cells were seeded and exposed to the EDCs or controls in transparent 96-well plates (TPP). Each treatment was conducted in triplicate wells. Total RNA was isolated following the Rneasy Plus Mini (QIAGEN, Hilden, Germany), with the samples from the triplicate wells pooled together. The quantity and quality of the total RNA were assessed by Nanodrop ND1000 spectrophotometer (Thermo Fisher). Reverse transcription was done using the cDNA Synthesis Kit (Meridian Biosciences, Cincinnati, OH), and qPCR was conducted with SensiFAST SYBR No-ROX Kit (Meridian Biosciences) on LightCycler II 480 (Roche, Basel, Switzerland). The qPCR conditions were as follows: initial activation for 2 min at 95 °C, followed by 40 cycles of denaturing for 5 s at 95 °C, annealing for 10 s at 55 °C and elongation for 20 s at 72 °C. The melting curve determination was started with denaturation (95 °C, 5 s), cooling (50 °C, 1 min), followed by continuous temperature rise (0.11 °C/s) to 95 °C. The primers were designed in Primer3, version 4.1.0 (Kõressaar et al., 2018), and are provided in Supplementary Material Table S1. Six biomarker genes involved in the KEs leading to imbalances in hepatic lipid homeostasis were analyzed (Angrish et al., 2016; Kubickova and Jacobs, 2023; Teixeira et al., 2023). Disruption of *de novo* lipogenesis was represented by *SREBF1* (encoding Sterol Regulatory Element-Binding Protein 1, a major transcription factor involved in the regulation of lipogenesis), *FASN* (encoding Fatty Acid Synthase, involved in fatty acid synthesis), and *DGAT1* (Diacylglycerol O-acyltransferase 1, involved in triglyceride synthesis). Fatty acid uptake was represented by *FAT/CD36* (Fatty Acid Translocase/Cluster of Differentiation 36). *CPT1A* (Carnitine Palmitoyltransferase 1A) facilitates mitochondrial transport and subsequent β-oxidation of fatty acids, while *APOB* (Apolipoprotein B) encodes a lipoprotein involved in hepatocellular lipid efflux. Cp values for the target genes were derived by the second derivative maximum ($2^{-\Delta\Delta CT}$) method (Livak and Schmittgen, 2001) and normalized to the geometric mean of two reference genes, *MDH1* and *EEF2* (Vandesompele et al., 2002). The reference-gene normalized data were then compared to the non-treated control and expressed as log2 fold change (log2 FC).

Statistical analysis. Normalized data from individual experiments (FOC or log2 FC) were combined, and the results are presented as means ± SEM from at least 3 independent experiments. Dose-response curve fitting was done using nonlinear regression models in GraphPad Prism v10 (Dotmatics, Boston, MA). To determine the integrative effects of EDCs on lipid accumulation over the tested concentration range, the

Area Under the Curve (AUC) was calculated using the trapezoid method. AUC values from the treatments were then normalized to the AUC value from the non-treated control and expressed as FOC. Aggregated changes in gene expression were calculated using the absolute values of log2 FC summed across the six evaluated target genes for each tested EDC or non-treated and solvent controls. Principal component analysis (PCA) was performed in GraphPad Prism v10 (Dotmatics). Other statistical analyses were done using Sigmaplot v12.3 software (Grafiti, Palo Alto, CA). Multiple group comparisons were made to determine significant differences from the control group using a one-way analysis of variance (ANOVA) for normally distributed data with equal variances. Non-parametric Kruskal Wallis ANOVA on ranks was used when assumptions of normality and homogeneity of variance were not met. A parametric *t*-test was used to evaluate the significance of differences in two group comparisons for normally distributed data with equal variances. For data that were not normally distributed or had unequal variances, the non-parametric Mann-Whitney test was used. Spearman's rank coefficient was calculated to characterize correlations between changes in gene expression and lipid accumulation. Values with $P < 0.05$ were considered as statistically significant.

3. Results

3.1. EDCs effects on cell viability

The effects of 10 selected EDCs were assessed for their 48-h impact on HepG2 cell viability to identify a non-cytotoxic concentration range for further experiments. This evaluation involved the MTT assay and, in parallel, a combination of three viability assays: resazurin (for metabolic activity of oxidoreductases and energy production), CFDA-AM (for esterase activity and membrane integrity), and NRU (for lysosomal uptake and retention of Neutral Red dye). The summary of the results is depicted in Fig. 1, with full concentration-response curves provided in Supplementary Material Figs. S1 and S2.

In the tested concentration range (from 0.1 nM to 100 μM), cytotoxic effects after 48 h exposure were observed for cadmium (≥10 μM), DDE, and BPA (at 100 μM). The estimated EC_{50} values for cadmium were 7 μM (MTT), 13 μM (resazurin), 18 μM (NRU) and 19 μM (CFDA-AM). DDE was less cytotoxic, inducing more than 50% reduction in cell viability only in NRU (EC_{50}~79 μM) and MTT (EC_{50}~97 μM) assays, while viability was non-significantly reduced to 52% or 67% of the control in the cells treated with 100 μM according to the CFDA-AM and resazurin assay (Fig. 1 and Fig. S1). BPA significantly reduced NRU and MTT conversion at 100 μM to 63% (NRU) or 70% (MTT) of the control, while the effects on resazurin and CFDA-AM conversion were less pronounced and not statistically significant (Fig. 1 and Fig. S2). Interestingly, DEHP increased esterase-dependent cleavage of CFDA-AM starting at a concentration of 10 μM (Fig. 1 and Fig. S2).

As five out of the 10 EDCs (cadmium, DDE, BPA, BPF, DEHP) affected cell viability at 100 μM, we decided to exclude the highest concentration from further testing, to focus on the conditions mimicking simple steatosis/MASL without a liver cell injury. We also evaluated the effects of these five EDCs, along with BPS, after a prolonged 6-day (144 h) exposure using RTCA followed by the NRU assay. Only cadmium significantly reduced cell impedance from the beginning of the exposure in a clear concentration- and time-dependent manner, with significant effects observed at 10–25 μM (Supplementary Material Fig. S3). This corresponded to the results of NRU assay, with an estimated 144-h-EC_{50} value of 9 μM (Supplementary Material Fig. S4). The other EDCs did not significantly inhibit the cell responses over time in the RTCA assay, except for a drop in impedance caused by BPA at 1 nM (Figs. S3 and S4). Interestingly, bisphenols induced non-monotonic responses in RTCA. BPA reduced impedance at concentrations of 0.1–1 nM, while BPS (0.1–1 nM) and BPF (10–25 μM) caused an increase in the signal after prolonged exposures.

In addition to EDCs, cell viability was also evaluated in response to amiodarone, a drug with known lipogenic effects, used as a positive control for lipid accumulation. Short-term treatment with amiodarone at 25–100 μM significantly reduced cell viability (EC_{50} values between 19 and 27 μM, Supplementary Material Fig. S5a). Concentrations 10–25 μM significantly reduced cell impedance (Supplementary Material Fig. S5b). The deleterious effect of 25 μM treatment persisted, and the cells did not recover. In contrast, cell impedance at 10 μM initially dropped by 25% between 24 and 48 h but started to recover after 45–50 h, eventually reaching control levels by 120 h. This was corroborated by NRU assessment after 144 h, showing a significant inhibition only at 25 μM (Supplementary Material Fig. S5c).

3.2. EDCs effects on lipid accumulation

Following cytotoxicity evaluation, the effects of EDCs on hepatic lipid accumulation, a KE in hepatic steatosis, were assessed after 48-h

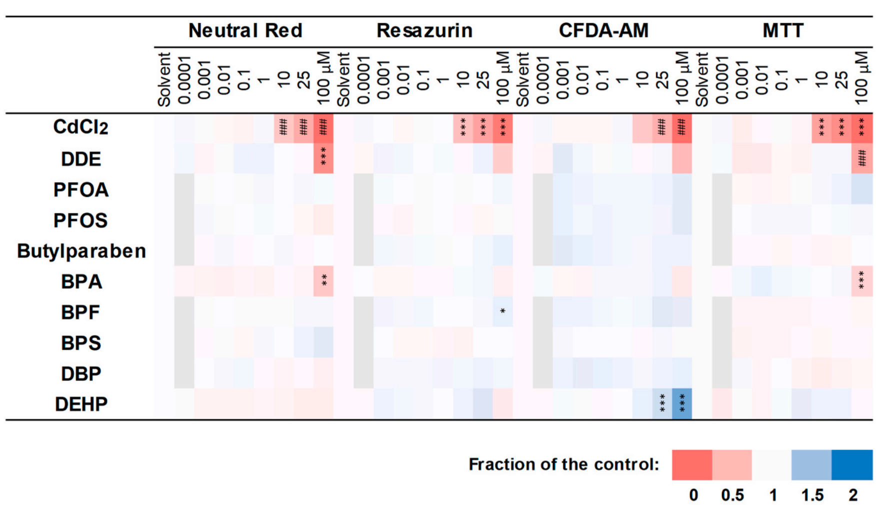

Fig. 1. Effects of EDCs on the viability of HepG2 cells after 48-h exposure. Viability was evaluated by Neutral Red uptake, Resazurin, CFDA-AM, and MTT. Data were normalized to the non-treated control and expressed as a fraction of the control (FOC). Data represent means from independently repeated experiments (n ≥ 3). Statistical significance was determined by comparison with the solvent control (0.1% DMSO, v/v) using ANOVA and Dunnett's test (*P < 0.05, **P < 0.01, ***P < 0.001) or non-parametric Kruskal Wallis ANOVA and Dunn's test when criteria of normality and homogeneity of variance were not met (#P < 0.05, ##P < 0.01, ###P < 0.001). (For interpretation of the references to colour in this figure legend, the reader is referred to the Web version of this article.)

exposure. This was done using a method utilizing staining of lipid droplets in HepG2 cells with Bodipy 493/503 dye and nuclei counter-staining with DAPI, followed by automated microscopic imaging and image analysis. The performance of this method was verified by assessing compounds with previously reported steatogenic effects (positive compounds), as well as chemicals not recognized to have significant effects on lipid accumulation (negative compounds). The results for selected experimental concentrations of positive and negative compounds are presented in Fig. 2. Concentration-response curves are provided in Supplementary Material Figs. S6 and S7, while representative microscopic images are shown in Fig. S8. The negative compounds, including anthracene, ascorbic acid, caffeine, caprolactam, and mannitol, did not affect lipid droplet formation at concentrations up to 100–1000 μM (Fig. S7). Fatty acids (PAOA, ≥50 μM), amiodarone (≥10 μM), chloroquine (≥25 μM), TBT (≥10 nM), etoposide (≥1 μM), TCS (≥10 μM), DINCH (≥25 μM), RGZ (≥10 μM, Fig. S6) and also TMPP (10 μM, Fig. S9) induced a significant increase in lipid accumulation after 48-h exposure. Lipid droplet formation significantly increased several-fold in response to PAOA, amiodarone, chloroquine, TBT, etoposide, TCS, and TMPP. In contrast, DINCH and RGZ led to a more moderate lipid accumulation, with up to 1.3- to 1.4-fold increase. PAOA (≤200 μM), TBT (10–100 nM), TMPP (≤10 μM), DINCH, and RGZ (≤25 μM) induced lipid accumulation at concentrations that did not affect cell density (Figs. S6 and S9). However, lipid accumulation caused by amiodarone, chloroquine, etoposide, and TCS was associated with a significant reduction in cell density relative to the control, due to inhibitory effects on cell proliferation and viability. At the lowest effective concentration inducing lipid accumulation, these compounds reduced cell density by approximately 25–60%. A decrease below the initial cell seeding density (i.e., below 40,000 cells/cm^2, approximately <0.2 FOC), indicating major cytotoxic effects associated with cell loss, was observed only for amiodarone at 25 μM, chloroquine at 50 μM, etoposide at 100 μM, and TBT at concentrations ≥1 μM (Fig. S6). Based on these results, 200 μM PAOA, 10 μM amiodarone, and 10 μM TMPP were selected as positive controls in each experiment testing EDCs for lipid accumulation. The summary of the positive controls for lipid

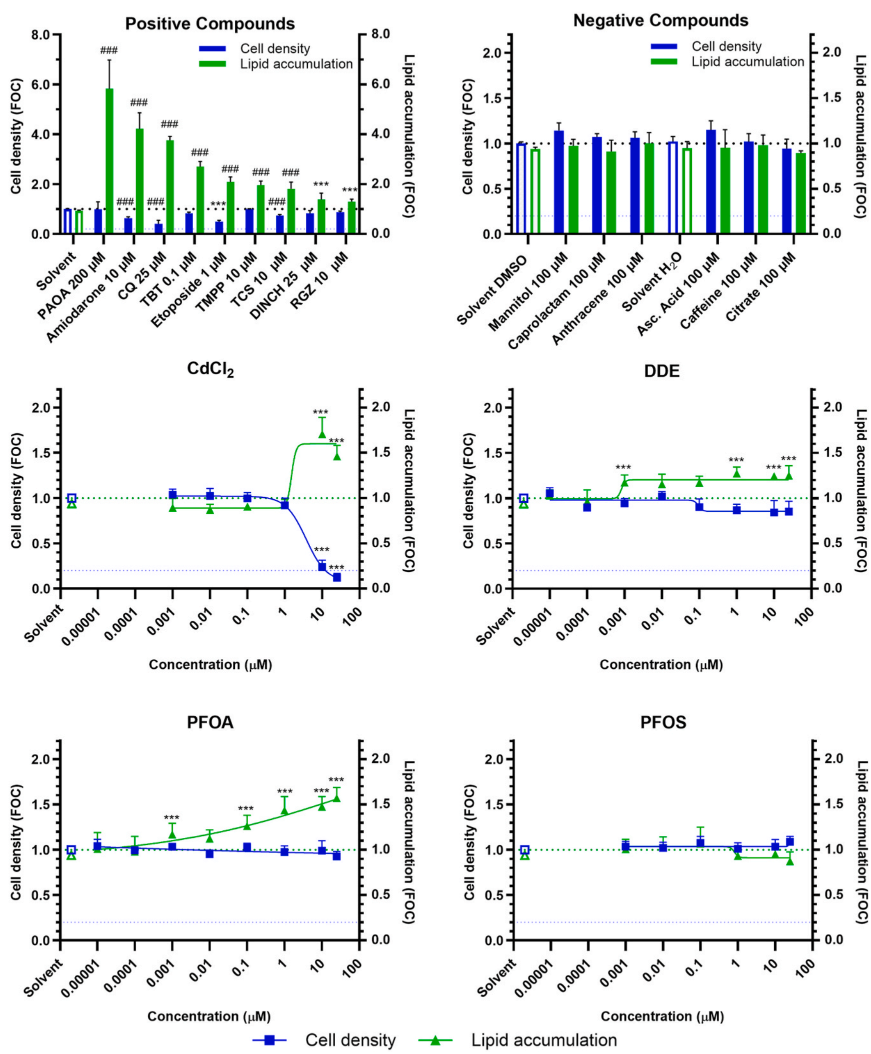

Fig. 2. Effects of model compounds and four studied EDCs on lipid accumulation in HepG2 cells after 48-h exposure. Cell density (DAPI-stained nuclei count per area) and lipid accumulation (integrated fluorescence of Bodipy 493/503-stained lipid droplets per nuclei count) were compared to the non-treated control and expressed as a fraction of the control (FOC). The dotted line(s) indicate(s) the non-treated control (FOC = 1.0). The fine dotted line indicates FOC = 0.2 for the cell density. Data represent means ± SEM from independently repeated experiments (n ≥ 3). More detailed concentration-response data for positive and negative compounds are available in Supplementary Material Figs. S6 and S7. Statistical significance was determined by comparison with the solvent control (0.1% DMSO, v/v, except for ascorbic acid, caffeine, and citrate, which used 0.1% water, v/v) using ANOVA and Dunnett's test (*P < 0.05, **P < 0.01, ***P < 0.001) or non-parametric Kruskal Wallis ANOVA and Dunn's test when criteria of normality and homogeneity of variance were not met (#P < 0.05, ##P < 0.01, ###P < 0.001). PAOA: palmitic:oleic acid mixture (1:2), CQ: chloroquine, TBT: tributyltin, TMPP: tris(methylphenyl) phosphate, TCS: triclosan, DINCH: 1,2-cyclohexane dicarboxylic acid diisononyl ester, RGZ: rosiglitazone, Asc. Acid: ascorbic acid.

accumulation from experiments with EDCs is given in Supplementary Material Fig. S9.

The effects of 10 selected EDCs are presented in Figs. 2 and 3. While exposures to PFOS, BPA, BPS, or DBP were not effective, cadmium significantly increased lipid accumulation at concentrations ≥10 μM, up to 1.5–1.7-fold of the control. However, this effect was associated with a reduction in cell density below 0.25 FOC, consistent with the results from the cell viability assays and RTCA. Other studied EDCs induced lipid accumulation at non-cytotoxic doses. DEHP increased lipid accumulation in a concentration-dependent manner, surpassing control levels by >20% at 1 μM and becoming significant at concentrations ≥10 μM, where it reached 1.3–1.7-fold of the control. Lipid droplet staining was also increased by PFOA, BPF, butylparaben, and DDE. Minor (<1.2-fold) but significant increases were occasionally observed at 1 nM concentration. However, effects became more pronounced (>1.25-fold increase) and consistently statistically significant at concentrations ≥100 nM for PFOA, BPF, and butylparaben, and ≥1 μM for DDE, as represented in Figs. 2 and 3.

The quantitative results in Figs. 2 and 3 are supported by the representative microphotographs for selected experimental concentrations of EDCs presented in Fig. 4, compared to non-treated control, solvent control, and positive controls (PAOA 200 μM, amiodarone 10 μM and TMPP 10 μM). As mentioned above, lipid droplet staining in response to PFOS, BPA, BPS, and DBP remained at levels comparable to the solvent control. In contrast, other EDCs clearly increased lipid accumulation at non-cytotoxic concentrations of 1–10 μM, except for cadmium, where the lipid droplet induction occurred at 10 μM concentration associated with cytotoxicity and a reduction in cell density.

3.3. EDC effects on expression of lipid metabolism-related genes

Since six out of 10 EDCs significantly induced lipid accumulation in HepG2 cells, we further examined their effects on the expression of representative genes involved in: 1) *de novo* lipogenesis (*SREBF1*, *FASN*, *DGAT1*), 2) hepatocellular uptake of fatty acids (*FAT/CD36*), 3) fatty acid oxidation (*CPT1A*), and 4) lipoprotein-mediated lipid efflux (*APOB*). The expression of these selected genes was first measured by RT-qPCR in cells exposed to positive control chemicals (Fig. S10). These chemicals that induced lipid accumulation also caused significant alterations in the gene expression. Amiodarone upregulated *FASN* and *CPT1A* while reducing *FAT/CD36*. PAOA significantly upregulated *DGAT1* and *CPT1A*, and also insignificantly increased the expression of

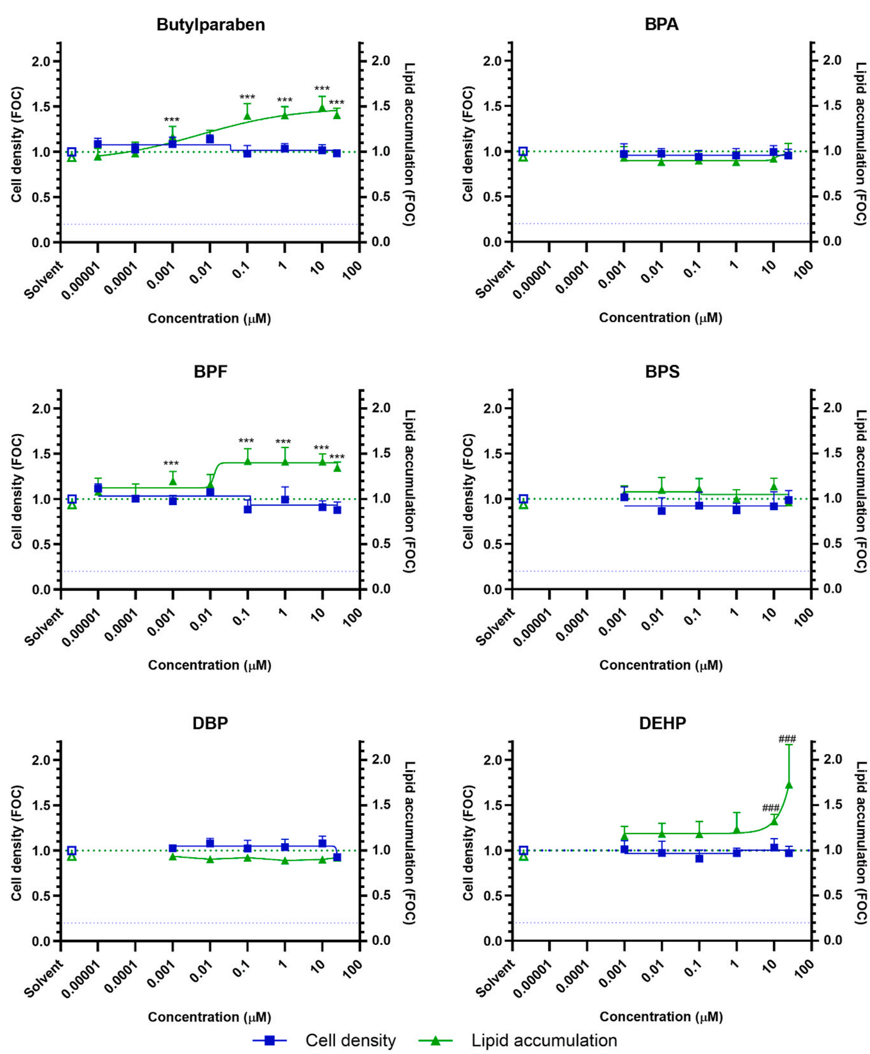

Fig. 3. Effects of six studied EDCs on lipid accumulation in HepG2 cells after 48-h exposure. Cell density (DAPI-stained nuclei count per area) and lipid accumulation (integrated fluorescence of Bodipy 493/503-stained lipid droplets per nuclei count) were compared to the non-treated control and expressed as a fraction of the control (FOC). The dotted line(s) indicate(s) the non-treated control (FOC = 1.0). The fine dotted line indicates FOC = 0.2 for the cell density. Data represent means ± SEM from independently repeated experiments (n ≥ 3). Statistical significance was determined by comparison with the solvent control (0.1% DMSO, v/v) using ANOVA and Dunnett's test (*P < 0.05, **P < 0.01, ***P < 0.001) or non-parametric Kruskal Wallis ANOVA and Dunnett's test when criteria of normality and homogeneity of variance were not met (#P < 0.05, ##P < 0.01, ###P < 0.001).

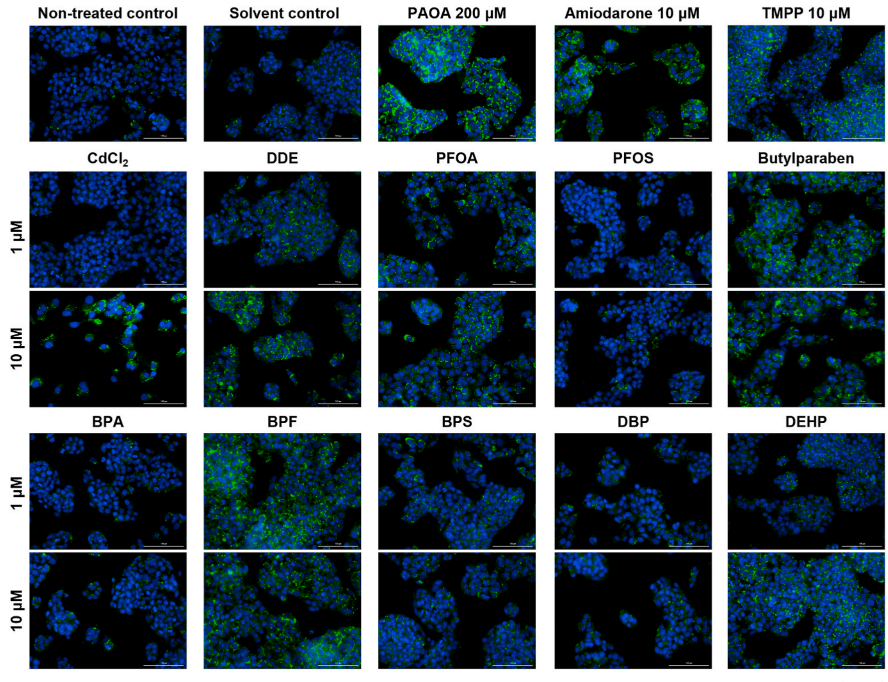

Fig. 4. Microphotographs of lipid droplet staining in HepG2 cells exposed to EDCs for 48 h. Representative images for selected concentrations (1 and 10 μM) of EDCs are shown alongside non-treated, solvent (0.1% DMSO, v/v), and positive controls (PAOA, amiodarone, TMPP). Lipids were stained with Bodipy 493/503 (green), and nuclei were counterstained with DAPI (blue). Images were acquired with a BioTek Cytation 5 imaging reader using a 20 × objective. Scale bar represents 100 μm. PAOA: palmitic:oleic acid mixture (1:2), TMPP: tris(methylphenyl) phosphate. (For interpretation of the references to colour in this figure legend, the reader is referred to the Web version of this article.)

SREBF1. TMPP also caused only an insignificant upregulation of *SREBF1* but significantly reduced the expression of *CPT1A*. In contrast, another negative control, represented by treatment with 0.1% (v/v) water, did not induce any significant changes in the expression of the selected genes. In aggregate, the changes in the expression of the selected genes increased for these lipid accumulation-inducing treatments when compared to non-treated or solvent controls (Fig. S10b).

For EDCs, our goal was to evaluate and compare their effects on gene expression at the same non-cytotoxic concentration for all tested compoudns. We selected a 1 μM concentration which did not alter cell viability for any compound. At this concentration, DDE, PFOA, butylparaben, BPF, and DEHP showed a 20–40% increase in lipid accumulation. In contrast, the other compounds, exept cadmium, did not alter lipid accumulation and remained at the control levels, even at concentrations up to 25 μM. For cadmium, the 1 μM concentration only preceded the lipid accumulation-inducing range (>1 μM), but these higher concentrations caused a significant reduction of cell counts and were therefore not considered for gene expression analysis. The results presented in Fig. 5 showed that the lipid accumulation-inducing EDCs also caused significant changes in the expression of the studied genes, while the effects of other compounds were not observed, except for BPA (more detailed results are presented in Supplementary Material Figs. S11 and S12). Most importantly, cadmium, DDE, PFOA, and DEHP induced the overexpression of *DGAT1*. Expression of this gene significantly correlated with the overall ability of the tested EDCs to induce lipid accumulation (Fig. 6). Similarly, the expression of *SREBF1* in response to EDCs significantly positively correlated with the effects on lipid droplet formation, with the six most potent inducers of lipid droplets causing the highest increase in *SREBF1* expression. In contrast, BPA reduced *SREBF1* expression to log2 FC of −0.5 (Fig. 6). Expression of *FASN* was not significantly changed by any of the EDCs (Fig. 5). *FAT/CD36* expression was significantly upregulated by exposure to butylparaben (Fig. 5). We also observed a significant inhibition of *CPTA1* expression by BPA. Cadmium rather increased *CPT1A* expression, although the effect was

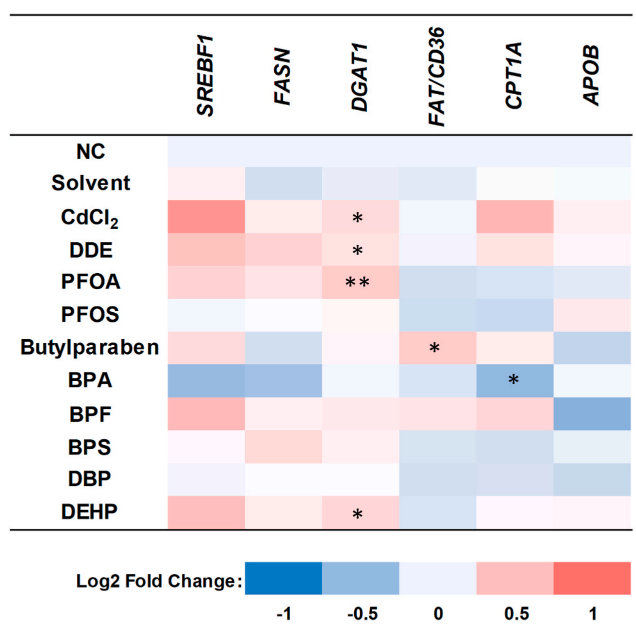

Fig. 5. Effects of EDCs on selected lipid metabolism-related genes in HepG2 cells exposed for 48 h. Gene expression was evaluated by RT-qPCR in the cells exposed to 1 μM EDCs. Reference gene-normalized data were expressed as a log2 fold change relative to the non-treated control. Data represent means from independently repeated experiments (n ≥ 3). Statistical significance was determined by comparison with the solvent control (0.1% DMSO, v/v) using a *t*-test (*P < 0.05, **P < 0.01, ***P < 0.001) or non-parametric Mann Whitney test when criteria of homogeneity of variance were not met (no significance found). (For interpretation of the references to colour in this figure legend, the reader is referred to the Web version of this article.)

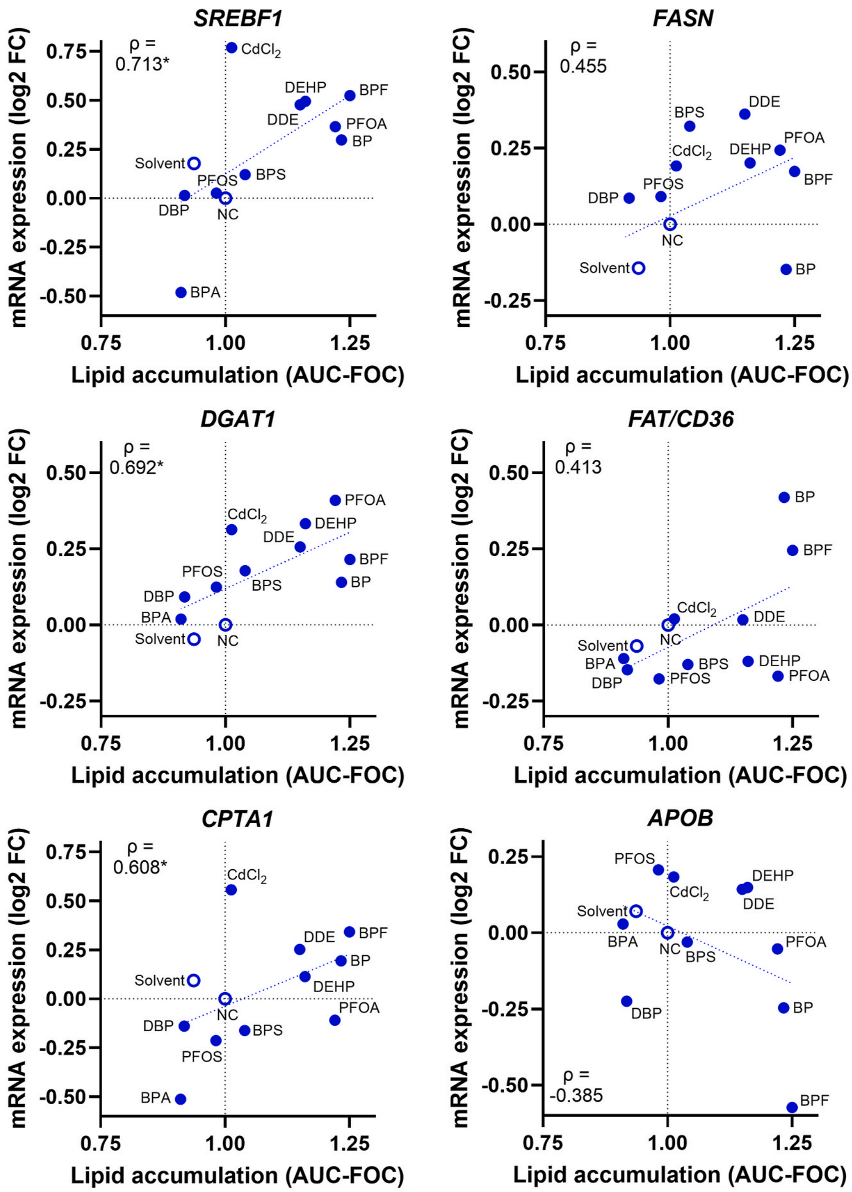

Fig. 6. Relationship between expression of lipid metabolism-related genes and lipid accumulation in HepG2 cells exposed to EDCs for 48 h. Reference gene-normalized RT-qPCR data for individual genes in response to 1 μM EDCs were expressed as a log2 fold change (log2 FC) relative to the non-treated control (log2 FC = 0.0). Lipid accumulation represents the area under the curve (AUC) from the concentration-response experiments, normalized to the non-treated control and expressed as a fraction of the control (FOC). Solvent: solvent control (0.1% DMSO, v/v), NC: non-treated control, ρ = Spearman's rank correlation coefficient, *P < 0.05.

not statistically significant (Fig. 5). However, the expression of this gene correlated significantly positively with lipid accumulation (Fig. 6). On the other hand, the expression of *APOB* exhibited a negative but insignificant correlation with lipid accumulation. The most pronounced inhibitory effect on *APOB* expression was observed for BPF (Fig. 6). The expression of *SREBF1*, *FASN*, and *DGAT1* significantly positively correlated with each other, while *CPT1A* also correlated with *SREBF1* and *FAT/CD36* expression. (Supplementary Material Fig. S13). Overall, the aggregated changes in all selected gene expressions increased with lipid accumulation, though the correlation was not significant (Fig. 7a). This relationship was most evident for the strongest inducers of lipid droplets, namely DDE, PFOA, butylparaben, BPF, and DEHP. However, a notable increase in aggregated gene perturbations was also observed for BPA and cadmium, reaching levels approximately two-fold higher than the solvent control. In contrast, PFOS, BPS, and DBP did not show significant changes, remaining at the solvent control level for both lipid droplets and gene expression. These relationships were also evident from PCA, which showed that lipid accumulation and aggregated gene expression were highly correlated parameters, that also clustered with *CPT1A*, *SREBF1*, *DGAT1*, and *FASN*. In contrast, less association was observed for *FAT/CD36*, and an opposite relationship was noted with *APOB* (Fig. 7b). Among EDCs, lipid accumulation-inducing DDE, PFOA, DEHP, and cadmium, which exhibited similar gene expression profiles, were grouped together. These four compounds were separate from lipid droplet-inducing butylparaben and BPF that affected mainly *FAT/CD36* and *APOB* expression, and apart from BPA. Compounds that did not induce significant effects (PFOS, BPS and DBP) were closest to the non-treated and solvent control (Fig. 7c).

4. Discussion

The current global rise in metabolic disorders, including MASLD, is

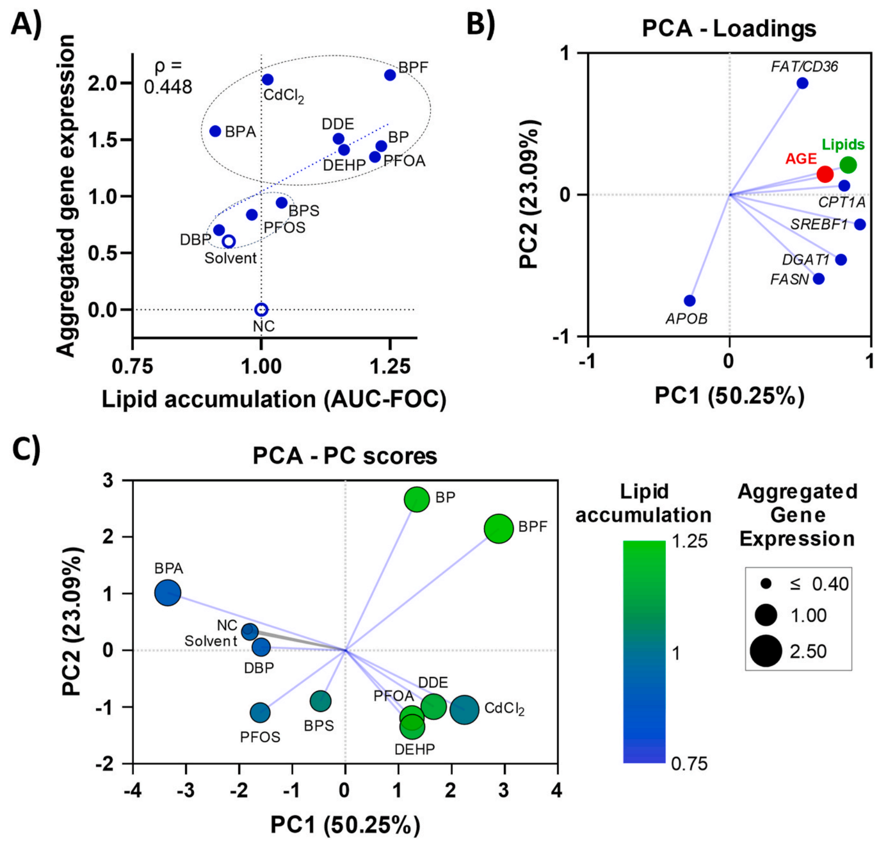

Fig. 7. Multivariate analysis of the relationship between the expression of lipid metabolism-related genes and lipid accumulation in HepG2 cells exposed to EDCs for 48 h. (A) Absolute values of log2 fold changes in the expression of six selected genes (*SREBF1*, *FASN*, *DGAT1*, *FAT/CD36*, *CPT1A* and *APOB*) were summed for individual EDCs. Lipid accumulation represents the area under the curve (AUC) from the concentration-response experiments normalized to the non-treated control (fraction of the control, FOC). Circles label chemicals inducing lipid droplet accumulation and/or dysregulating lipid metabolism genes vs. chemicals without such effects. (B–C) Principal Component Analysis (PCA) of the expression of six selected genes, aggregated changes in the gene expression (AGE), and lipid accumulation (Lipids). Solvent: solvent control (0.1% DMSO, v/v), NC: non-treated control, ρ = Spearman's rank correlation coefficient.

not solely attributed to dietary, lifestyle, and genetic factors but also to environmental chemical exposures. EDCs, which interfere with metabolic functions and act as MDCs, are increasingly recognized as health hazards contributing to hepatic steatosis and MASLD (Cano et al., 2021; Fritsche et al., 2023; Heindel et al., 2017, 2022; Mosca et al., 2024). Investigating EDC mechanisms and developing effective tools for assessing their steatogenic potential is a critical research and regulatory priority to support public health protection through informed regulatory and policy measures (Audouze et al., 2020; Küblbeck et al., 2020; Legler et al., 2020).

In this study, we investigated the impact of selected EDCs on key processes involved in hepatic steatosis using an *in vitro* HepG2 model. Ten chemicals were selected to represent major EDC groups of regulatory and public health interest (Audouze et al., 2020). The *in vitro* model based on a human HepG2 cell line was combined with neutral lipid droplet staining using Bodipy 493/503, quantified through automated imaging and image analysis in a 96-well microplate setup (Donato et al., 2012; Tolosa et al., 2012). This method has previously identified steatogenic effects of drugs, though with smaller responses compared to more complex models like differentiated HepaRG cells (Tolosa et al., 2016). Here, we employed a modified protocol without fatty acid overloading, similar to other studies examining lipid accumulation and steatosis-relevant KEs in HepG2 cells in response to various EDCs (Lin et al., 2017; Liu et al., 2020; Negi et al., 2021; Peyre et al., 2014; Wen et al., 2020). Evaluating changes in the basal number and size of lipid droplets without fatty acid overloading could enhance the detection of subtle variations.

To evaluate the performance of the method, we assessed a set of chemicals linked to MASLD and known to induce lipid droplets and accumulation in human hepatic cell lines *in vitro*. A binary mixture of palmitic:oleic acid (1:2) is a well-established inducer of hepatic steatosis both *in vitro* and *in vivo* (Kubickova and Jacobs, 2023). It has been found to cause a lipid accumulation in HepG2 cells at concentrations up to 200 μM without causing cytotoxicity, which would represent conditions observed in chronic benign or mild steatosis (Campos-Espinosa and Guzmán, 2021; Gómez-Lechón et al., 2007). Amiodarone, a cationic amphiphilic drug used to treat arrhythmia, represents a known inducer of hepatic steatosis and phospholipidosis (Kubickova and Jacobs, 2023). Here, it induced lipid accumulation in HepG2 cells at (sub)cytotoxic concentrations (10–25 μM), in agreement with previous studies (Donato et al., 2012; Grünig et al., 2018). Chloroquine, another cationic amphiphilic drug used for malaria treatment, is a recognized inducer of phospholipidosis (Donato et al., 2022). It has been reported to increase both phospholipid and neutral lipid content in HepG2 cells (Park et al., 2012), which corresponds to our results.

TBT, a fungicide with obesogenic activity, induced hepatic lipid accumulation *in vivo* and *in vitro* (Fritsche et al., 2023; Kubickova and Jacobs, 2023), including in HepG2 and HepaRG cells. PPARγ/RXRα-dependent lipid accumulation was induced by nanomolar (5–50 nM) concentrations, while concentrations above 100 nM became cytotoxic (Franco et al., 2020; Stossi et al., 2019), similar to our findings. Etoposide, an anticancer agent causing apoptosis and senescence, caused at a concentration of 20 μM lipid accumulation in HepG2 cells and immortalized human hepatocytes, disrupted lipid and glucose metabolism, and promoted other MASLD markers, which was further exacerbated by oleic acid overloading (Bonnet et al., 2022). These results correspond to our observations. TCS, an antifungal and antimicrobial compound used in personal care products, is known to interact with xenobiotic receptors and induce oxidative stress. TCS was found to exacerbate high-fat diet-induced hepatic steatosis in mice (Yueh et al., 2020) and to induce liver injury accompanied by the formation of lipid droplets and hepatic steatosis in standard-fed mice (Song et al., 2022). *In vitro*, TCS differentially dysregulated lipid metabolism in L02 and HepG2 cells (Zhang et al., 2019). However, the transcriptomic profiles of TCS-exposed primary human hepatocyte spheroids did not align with the predicted response for steatosis or fibrosis (Vilas-Boas et al., 2021). Thus, the observed increase in lipid droplets in our study could facilitate further research to clarify uncertainties regarding the ability of TCS to affect MASLD (Kubickova and Jacobs, 2023).

TMPP is a novel flame retardant structurally similar to triphenyl phosphate (TPHP). TPHP has been previously found to induce hepatic steatosis *in vivo* (Cui et al., 2022; Wang et al., 2019), as well as triglyceride or lipid droplet accumulation *in vitro* in HepG2 cells at concentrations of 1–50 μM (An et al., 2023; Hao et al., 2019; Xiang and Wang, 2021). TMPP induced similar effects to TPHP in HepG2 cells *in vitro*, including a shared PPARγ/PXR-mediated mechanism of action (Hao et al., 2019; Negi et al., 2021; Yu et al., 2024). DINCH, a plasticizer substituting for phthalates, disrupted lipid transport and homeostasis in zebrafish larvae (Saad et al., 2021). It also induces adipogenesis in murine 3T3-L1 preadipocytes (Bereketoglu et al., 2024). The DINCH metabolite, cyclohexane-1,2-dicarboxylic acid monoisononyl ester (MINCH), activates PPARγ, inducing lipid accumulation and adipogenesis in human SGBS preadipocytes at concentrations of 5–10 μM, similar to RGZ (Schaffert et al., 2022). In mature SGBS adipocytes, both DINCH and MINCH induced oxidative stress and impaired lipid metabolism and storage (Schaffert et al., 2022). Recently, transient oxidative DNA damage without cytotoxicity was reported in HepG2 cells exposed to ≥2 μM DINCH (Vasconcelos et al., 2019). Our study thus provides new evidence that non-cytotoxic concentrations of DINCH can also disrupt lipid homeostasis and induce lipid accumulation in human hepatic cells. RGZ, an antidiabetic drug, decreased hepatic lipid accumulation and reduced steatohepatitis in patients (Kubickova and Jacobs, 2023). Correspondingly, RGZ reduced lipid accumulation after a long-term (14 days) treatment of oleic acid-overloaded HepaRG cells (Rogue et al., 2014). However, the effects of RGZ are more complex, since this potent PPARγ agonist acts as an obesogen and was reported to induce hepatic steatosis in rodent studies (Kubickova and Jacobs, 2023). In HepaRG cells, 10 nM-1 μM RGZ increased total lipid content and induced neutral lipid droplet formation without impairing cell viability (Franco et al., 2020). This is consistent with our findings, where similar effects on lipid droplets were observed at non-cytotoxic RGZ concentrations of 10 nM–25 μM. On the other hand, chemicals not known to be hepatotoxic and not inducing hepatic steatosis, such as mannitol, caprolactam, anthracene, citrate, ascorbic acid or caffeine (Kubickova and Jacobs, 2023; Tolosa et al., 2016) did not increase lipid droplets in HepG2 cells in our study. In agreement with previous research, we observed that lipid accumulation induced by PAOA (Liu et al., 2022; Qi et al., 2020; Ren et al., 2024), amiodarone (Donato and Goméz-Lechón, 2012) or TMPP (Hao et al., 2019; Negi et al., 2021), was generally associated with perturbations in the expression of lipid metabolism-related genes evaluated in our study, in contrast to non-treated and solvent controls. This suggests that the *in vitro* model used in our study was effective in detecting disruption of lipid metabolism in human hepatic cells induced by steatogenic compounds with varied modes of action in conditions without fatty acid overloading.

Consequently, the model was used to assess the effects of 10 selected EDCs at non-cytotoxic concentrations (i.e., ≤1 μM cadmium and ≤25 μM for the others), covering 0.1–100 nM concentrations relevant for chronic human internal exposures (Chen et al., 2023; Le Mentec et al., 2023; Sadrabadi et al., 2024). Our findings reveal that five chemicals (DDE, PFOA, butylparaben, BPF, and DEHP) significantly increased lipid droplet accumulation at non-cytotoxic concentrations, primarily at ≥1 nM. Although cadmium increased lipid accumulation at >1 μM associated with cytotoxicity, it altered the expression of lipid metabolism-related genes at a non-cytotoxic 1 μM concentration. BPA at 1 μM affected gene expression without detectable changes in lipid droplet accumulation.

A significant finding from our investigation is that, under the same experimental conditions, the EDCs inducing lipid accumulation increased *DGAT1* expression, particularly cadmium, DDE, PFOA, and DEHP, indicating enhanced triglyceride synthesis. Additionally, *DGAT1* expression in response to EDCs was positively correlated with the expression of *SREBF1*, a major regulator of lipid metabolism, as well as *FASN*, which is involved in fatty acid synthesis (Angrish et al., 2016; Bernal et al., 2022). This suggests that stimulation of *de novo* lipogenesis was a major mechanism contributing to the accumulation of lipid droplets induced by EDCs. Interestingly, increased expression of *SREBF1* was mostly associated with the upregulation of the *CPT1A* gene responsible for the transportation of long-chain fatty acids into the mitochondria for β-oxidation (Angrish et al., 2016; Bernal et al., 2022). This might indicate increased fatty acid oxidation due to compensatory mechanisms by which liver cells attempt to manage lipid and lipotoxicity overload, as well as due to EDC interactions with multiple pathways regulating expression of these genes (Ipsen et al., 2018). Conversely, BPA significantly downregulated *CPT1A*, which could be potentially leading to hepatic steatosis due to reduced fatty acid oxidation. Butylparaben upregulated *FAT/CD36* gene coding a transmembrane glycoprotein involved in the uptake of long-chain fatty acids into cells (Angrish et al., 2016; Bernal et al., 2022). Consequently, increased uptake of fatty acids can contribute to the accumulation of lipid droplets within hepatic cells, ultimately leading to steatosis (Miquilena-Colina et al., 2011; Sheedfar et al., 2014; Rada et al., 2020). Finally, downregulation of the *APOB* gene encoding apolipoprotein B involved in the hepatocellular efflux of lipids was most pronounced with BPF and can also lead to increased hepatocellular lipid accumulation (Angrish et al., 2016; Bernal et al., 2022). Although the *APOB* expression change was insignificant, it appeared to be regulated in the opposite direction compared to *FAT/CD36* in response to both butylparaben and BPF. On the other hand, PFOS, BPS, and DBP neither induced lipid droplets nor caused significant dysregulation of the selected genes. Consequently, their aggregated gene expression values remained close to the solvent control level. In contrast, the remaining seven EDCs, which included those inducing lipid droplets, resulted in more than a two-fold increase (cadmium, DDE, PFOA, butylparaben, BPA, BPF, DEHP). Observations of these effects at non-cytotoxic concentrations indicate that exposures to these EDCs could contribute to the development of simple steatosis without causing cell injury.

Importantly, these effects were observed without fatty acid overloading, highlighting the ability of EDCs to induce steatosis rather than promote or aggravate it, which is typically modeled with pre- or co-exposures to fatty acids (Bernal et al., 2024). These results partially align with previous *in vitro* studies employing diverse cell models and experimental settings while also providing novel observations. Per-/-polyfluoroalkyl substances (PFAS) are synthetic chemicals used in a variety of industrial applications and consumer products and are among the most studied groups of environmental toxicants linked to MASLD (Fragki et al., 2021; Fritsche et al., 2023; Kowalczyk et al., 2023; Kubickova and Jacobs, 2023). Similarly to our study, Qi et al. (2023) reported the induction of lipid accumulation by PFOA (10–100 nM) in both HepG2 and HepaRG cells after 48 h of exposure, with oleic acid co-exposure during the last 24 h of PFOA treatment (Qi et al., 2023). PFOA also upregulated the expression of *SREBF1* in HepG2 cells and *SREBF1* and *FASN* in HepaRG cells, along with other cellular changes linked to unfolded protein response, ROS production, steatosis, inflammation, and fibrosis (Qi et al., 2023). PFOA (10–50 μM, 48 h) also induced autophagy and increased the levels of SREBP1c protein and several enzymes involved in fatty acid synthesis (FAS, ACC, SCD1) in human L02 cells (Weng et al., 2020). In HepG2/C3A cells, PFOA

(20–200 μM, 48 h) caused concentration-dependent upregulation in the expression of genes involved in long-chain fatty acid activation (*ACSL1*) but inhibited expression of genes involved in fatty acid uptake (*FABP1*), degradation (*ACOX2*) or cholesterol synthesis (*HMGCR*) (Wen et al., 2020). This pattern aligns with our findings, indicating that lipid droplet accumulation in response to PFOA was mediated by increased lipogenesis genes (*DGAT1*, *SREBF1*) without major impacts on the expression of genes involved in fatty acid uptake, oxidation, or efflux (*FAT/CD36*, *CPT1A,* and *APOB*). A recent study showed increased accumulation of lipids by PFOS in HepG2 cells via the AMPK-ACC pathway (Ling et al., 2023) but at a much higher concentration (150 μM, 48 h) than used in our study, where PFOS did not show steatogenic effects, unlike PFOA.

Several studies in HepaRG cells highlight distinctions between the effects of PFOA and PFOS. In line with our results, PFOA increased neutral lipid droplets (≥100 nM) and total lipid content (≥1 nM) after a 7-day exposure, while PFOS did not increase neutral lipid droplets and showed varying effects on cellular lipid levels (Franco et al., 2020). In another study, PFOA (250 μM, 72 h) but not PFOS increased triglyceride levels, although both altered the expression of gene markers for steatosis after 24-h exposure (Sadrabadi et al., 2024). In contrast, Louisse et al. (2020) reported that PFOS was a more potent inducer of triglyceride levels in HepaRG cells after 24-h exposure than PFOA, with 50% benchmark concentration values of 93 μM for PFOS and 184 μM for PFOA, respectively (Louisse et al., 2020). The transcriptomic analysis found PFOA more effectively activated PPARα-regulated genes, while PFOS more strongly inhibited cholesterogenic genes (Louisse et al., 2020). Another study showed that neither PFOA nor PFOS (up to 25 μM, 5-day exposure) induced lipid accumulation in monolayer HepaRG cultures regardless of the oleic acid supplementation, while 25 μM PFOA increased lipid droplets and triglyceride content in 14-day exposed 3D HepaRG cultures (Bernal et al., 2024). Although both PFOA and PFOS have been reported to dysregulate lipid metabolism in human liver cells *in vitro*, the varied experimental designs make a conclusive understanding challenging (Bernal et al., 2024). However, it appears that PFOA and PFOS each elicit distinct responses in hepatic cells, as observed in our study, where PFOA was a more potent inducer of steatosis-related markers than PFOS.

Bisphenols, used in plastic manufacturing, represent another group of EDCs implicated in the disruption of lipid metabolism. Studies on bisphenols, especially BPA, using human liver *in vitro* models show inconsistent results (Fritsche et al., 2023; Kowalczyk et al., 2023; Kubickova and Jacobs, 2023). For example, BPA induced oxidative stress and lipid droplets in HepG2 cells exposed to 1 pM-1 μM for 72 h (Huc et al., 2012). In contrast, triglyceride levels increased only at 1 pM BPA from a range of 1 fM-1 μM after 96 h of exposure (Héliès-Toussaint et al., 2014), while increased lipid droplet accumulation was observed only at ≥25 μM over 72 h (Peyre et al., 2014). The effects of 50 nM BPA on lipid accumulation and oxidative stress in HepG2 cells exposed for 48 h were conditioned by co-exposure to oleic acid or using a high-glucose culture medium (Dallio et al., 2018). Lin et al. (2017) reported that 20 nM-2 μM of BPA (48 h) gradually increased lipid accumulation and triglyceride levels in HepG2 cells and altered several genes involved in lipid metabolism, including upregulation of *SREBF1*, *FASN*, *FAT/CD36* or *APOB*, or downregulation of *DGAT1* (Lin et al., 2017). Liu et al. (2020) found lipid accumulation and gene expression changes in HepG2 cells exposed to 10 μM BPA for 24 h, including increased expression of lipogenesis genes (*FASN*, *ACC*, and *SCD1*) and inhibited expression of fatty acid oxidation-related genes like *CPT1A* (Liu et al., 2020). Downregulation of *CPT1A* by BPA was also observed in our study, but it was associated rather with a reduced expression of *SREBF1* and not accompanied with lipid accumulation. This is similar to the findings of Shimpi et al. (2017), who reported that 100 nM BPA did not show a significant increase in lipid accumulation and triglyceride levels in primary human hepatocytes and HepG2 cells, while reducing SREBP1c protein levels in hepatocytes and not activating the SREBP1c gene in transgenic HepG2 cells (Shimpi et al., 2017). In HepaRG cells, a 3-week exposure to 0.2–2000 nM BPA showed that only 2 nM dose increased neutral lipid accumulation, triglyceride levels, and transcription of lipid efflux-related gene *APOA4*, but not the expression of lipid droplet protein genes *PLIN2/3* (Bucher et al., 2017). In a shorter 7-day exposure of HepaRG cells, BPA enhanced total lipid content at 0.1–10 nM concentrations, decreasing to control levels at 100–1000 nM. Meanwhile, lipid droplets increased in an opposite manner between 10 and 1000 nM (Franco et al., 2020). Recently, exposure of HepaRG to 25 μM BPA and their analogues, BPF and BPS, with or without oleic acid supplementation, did not result in lipid accumulation in a monolayer setup, while 14-d exposure of 3D HepaRG to 10 μM BPA increased lipid droplets and triglyceride content (Bernal et al., 2024).

BPA-replacement analogues, such as BPS and BPF, also induce steatosis-related responses in human hepatic cells *in vitro*, supported by our study, with varying potencies and response patterns (Ferreira Azevedo et al., 2022; Héliès-Toussaint et al., 2014; Liu et al., 2020; Ozyurt et al., 2023; Peyre et al., 2014). BPS (1 fM-1 nM) was more potent than BPA in increasing triglyceride levels in HepG2 cells (Héliès-Toussaint et al., 2014), but lipid droplet staining showed BPS was effective only at 500 μM and BPA at ≥25 μM (Peyre et al., 2014). Liu et al. (2020) ranked the potency for lipid accumulation as BPA > BPF ≫> BPS (10 μM). BPS did not significantly affect the expression of genes involved in lipid metabolism (Liu et al., 2020), which aligns with our results. BPF (10 μM, 24 h) was a potent inducer of lipid accumulation and triglyceride content in HepG2 cells with low cytotoxicity (Liu et al., 2020; Wang et al., 2021). In our study, BPF was the most steatogenic bisphenol analogue, with respect to its low cytotoxicity, significant effects on lipid droplets, and substantial effect on the aggregated gene expression change, driven mainly by upregulation of *SREBF1* and downregulation of *APOB*. BPF was followed by BPA, the most cytotoxic bisphenol causing dysregulation of lipid metabolism-related genes, both individually (*CPT1A*) and in the aggregate, although without significant effects on lipid droplets in the studied concentration range. In contrast, BPS had low cytotoxicity and neither induced lipid accumulation nor affected the expression of lipid metabolism-related genes.

DEHP, a phthalate used as a plasticizer, is implicated in metabolic disruption (Fritsche et al., 2023; Heindel et al., 2022; Kowalczyk et al., 2023). *In vitro*, DEHP increased lipid droplets in HepG2 cells co-exposed with oleic acid for 48 h, along with higher PPARα and SREBP1c protein levels (Zhang et al., 2017). Similarly, DBP (100–200 μM, 48 h), with or without oleic acid overloading, increased lipid accumulation and expression of PPARα, SREBP1c, or FAS proteins in HepG2 cells via a PPARα/RXR dependent mechanism (Zhang et al., 2021). DEHP and DBP induced distinct effects on the transcriptomic and metabolic profiles of HepG2 cells, including alterations in carbohydrate and lipid metabolism; however, these changes occurred in response to relatively high concentrations of 10 mM (Dong et al., 2023). Lower DEHP concentrations increased lipid levels (1000 nM) and lipid droplet staining (10–1000 nM) in HepaRG cells exposed for 7 days (Franco et al., 2020). DEHP, but not DBP, increased lipid droplets in HepaRG cells exposed to 25 μM for 5 days, both with and without oleic acid co-exposure. DEHP effects on lipid droplets in the presence of oleic acid started from 1 μM and were accompanied by higher *PLIN2* expression and protein levels. This was confirmed in 3D HepaRG culture treated with 10 μM DEHP for 14 days (Bernal et al., 2024). Similarly, we observed increased lipid accumulation in response to DEHP but not DBP, suggesting that DEHP or its metabolites are more potent inducers of steatosis, mainly due to enhanced lipogenesis indicated by the upregulation of *DGAT1* and *SREBF1*.

Among organochlorine pesticides, DDE and its parental compound, DDT, are primarily studied for their effects on adipocytes and pancreatic cells (Heindel et al., 2022; Kowalczyk et al., 2023). However, less is known about DDE effects on human hepatic cells *in vitro*. DDE at 1–10 ng/mL (3–31 nM) increased lipid droplet staining and triglyceride levels in HepG2 cells exposed for 24 h, associated with the upregulation of genes and proteins involved in lipogenesis, such as *SREBF1*, *FAS*, and

SCD1, and the downregulation of genes and proteins involved in β-oxidation, such as *CPT1A*, *MCAD*, and *SCAD* (Ji et al., 2016; Liu et al., 2017). In HepaRG cells, DDE combined with oleic acid induced lipid droplet accumulation, with the effects increasing gradually from 1 to 25 μM. DDE also upregulated *PLIN2* and inhibited long-chain fatty acid oxidation but downregulated selected genes involved in lipogenesis, fatty acid and triglyceride synthesis (*SREBF1*, *SCD1*, *FASN*, *DGAT1*), fatty acid uptake (*FABP*) or lipid efflux (*MTTP*). Lipid accumulation was also observed in 3D cultures of HepaRG exposed to DDE for 14 days (Bernal et al., 2024). Our findings partly align with these results, showing increased lipid accumulation in HepG2 cells from 1 nM DDE, with elevated expression of *DGAT1* and *SREBF1* indicating enhanced lipogenesis.

Parabens, used as preservatives in pharmaceutical and personal care products, have less-studied effects on hepatic steatosis *in vitro* (Heindel et al., 2022; Kowalczyk et al., 2023). Co-exposure of oleic acid with 1 μM of methyl- or ethylparaben for 24 h increased lipid droplet staining and triglyceride and cholesterol levels in HepG2 cells, associated with higher expression of *SREBF1*, *FASN*, *ACC*, *CPT1A*, and *PLIN2* (Ren et al., 2024). Our findings revealed that butylparaben can induce lipid accumulation in HepG2 cells at ≥1 nM without fatty acid overloading, primarily upregulating *FAT/CD36* gene. However, butylparaben (25 μM, 5 days) did not induce lipid accumulation in HepaRG cells, with or without oleic acid overloading (Bernal et al., 2024).

Heavy metals, like cadmium, also act as obesogens and metabolic disrupters (Fritsche et al., 2023; Heindel et al., 2022; Kowalczyk et al., 2023). Cadmium (5–10 nM, 30 h) followed by oleic acid treatment increased lipid droplets in HepG2 and HepaRG cells, affecting genes and proteins involved in lipid metabolism, such as *SREBF1, ACC,* or *PPARγ* in both cell lines, with *FABP* increased only in HepaRG cells (Niture et al., 2023). Similarly, cadmium increased lipid droplet staining in undifferentiated HepaRG cells at 20–50 μM after 24-h exposure, exacerbated by 48-h fatty acid treatment (Migni et al., 2023). Also, 48-h exposure to 0.125–2 μM of cadmium increased triglyceride content in HepG2 cells (Kong et al., 2021). In contrast, cadmium did not increase triglyceride levels in HepG2 cells (10 μM, 24 h) or lipid droplets in HepaRG cells (25 μM, 5 days, with or without oleic acid) (Bernal et al., 2024; He et al., 2015). Our *in vitro* model supports that subcytotoxic cadmium concentrations upregulate lipogenesis and triglyceride synthesis genes (*DGAT1*, partially *SREBF1*), potentially leading to lipid accumulation and droplet formation at higher concentrations or after longer exposures.

There is growing evidence from *in vitro* studies that EDCs, including the compounds investigated here, can disrupt lipid metabolism and contribute to hepatic steatosis/MASLD. However, the specific effects observed in individual studies are sometimes inconsistent (Heindel et al., 2022; Kubickova and Jacobs, 2023). This inconsistency may be due to differences in cellular systems, culture conditions, experimental designs, treatment protocols, and detection methods, which are rarely harmonized across the different studies. Specific exposure concentrations and durations are critical, as EDCs exhibit non-monotonic dose responses (Vandenberg et al., 2012). These responses may result from impacts on multiple receptor-mediated pathways, including antagonistic effects with differing dose-response profiles, and effects on receptor number and turnover (Heindel et al., 2022). Furthermore, factors affecting the cellular system, such as cell type, culture conditions (e.g., glucose, fatty acid, growth factor, or hormone concentrations in the medium), and cell density or growth phase, can influence cell characteristics such as differentiation status, metabolic pathways, and the expression of receptors, transporters, or enzymes. These characteristics can affect cellular response to chemicals, including uptake, biotransformation, and interactions with respective molecular targets. The direction and magnitude of reported changes in the expression of lipid metabolism-related genes vary widely across studies, likely due to the complex regulation and dynamics of lipid and carbohydrate metabolism pathways disrupted by EDCs. Despite this variability, overall perturbations in genes involved in lipid homeostasis (Angrish et al., 2016; Bernal et al., 2022; Kubickova and Jacobs, 2023) are consistently observed alongside increased lipid accumulation in hepatic cells *in vitro* (Fritsche et al., 2023; Kowalczyk et al., 2023). Our study supports that evaluating these genes can serve as a reliable *in vitro* biomarker of steatogenic potential, even in simpler systems such as monolayer cultures of HepG2 cells. While these cultures do not fully replicate normal human hepatocytes and lack the complexity of advanced systems like 3D cultures (Arzumanian et al., 2021; Donato et al., 2022; Yang et al., 2023), some studies highlight the importance of metabolism-disrupting effects in different cell types of hepatocyte lineage, such as hepatoblasts or hepatic progenitors (Shimpi et al., 2017; Shree Harini and Ezhilarasan, 2023; Vanova et al., 2019). Thus, HepG2-based *in vitro* models may provide valuable insights into the steatogenic effects directly induced by MDCs in less differentiated hepatic cells. The approach utilized in this study can be useful for the initial screening and prioritization of MDCs, setting up exposure and time windows for more detailed mechanistic and omics studies, including those conducted in more complex *in vitro* models.

5. Conclusions

Our study demonstrates that several model steatogenic compounds and selected EDCs associated with metabolic disruption and MASLD affect key molecular and cellular events mechanistically linked to hepatic steatosis in an *in vitro* model of human hepatic cells HepG2. Although the effects of EDCs were relatively moderate, they were mostly induced at non-cytotoxic concentrations (≤1 μM) that did not affect cell viability or growth, mimicking conditions of simple steatosis without liver injury, inflammation, or hyperplasia. These effects were observed directly, without fatty acid overloading, and after a relatively short exposure time. Thus, this *in vitro* model offers a relatively simple, accessible, and easy-to-standardize system with sufficient throughput, enhanced by automated imaging and image analysis. It could meet regulatory needs for identifying chemical hazards and risks of metabolic disruption and MASLD caused by EDCs, emphasizing the reduction of animal testing in line with the 3Rs principles (Audouze et al., 2020). The paradigm is shifting towards using mechanistic knowledge in IATAs and incorporating NAMs like human-relevant, *in silico, in chemico,* and *in vitro* test methods, to support regulatory decisions (Kubickova and Jacobs, 2023). *In vitro* systems based on human hepatic cells could be valuable for early screening in testing strategies, complementing information from other methods, and eventually followed by more complex test systems for accurate health hazard and risk assessment.

CRediT authorship contribution statement

Marina F. Grosso: Writing – review & editing, Writing – original draft, Visualization, Validation, Methodology, Investigation, Funding acquisition, Formal analysis, Data curation, Conceptualization. **Eliška Řehůřková:** Writing – review & editing, Visualization, Validation, Methodology, Investigation, Formal analysis. **Ishita Virmani:** Writing – review & editing, Visualization, Validation, Methodology, Investigation, Formal analysis. **Eliška Sychrová:** Writing – review & editing, Visualization, Validation, Methodology, Investigation, Formal analysis. **Iva Sovadinová:** Writing – review & editing, Validation, Supervision, Resources, Methodology, Formal analysis. **Pavel Babica:** Writing – review & editing, Writing – original draft, Visualization, Supervision, Resources, Project administration, Methodology, Funding acquisition, Formal analysis, Data curation, Conceptualization.

Declaration of generative AI and AI-assisted technologies in the writing process

During the preparation of this work the authors used Microsoft Copilot to enhance language quality and clarity. After using this tool, the authors reviewed and edited the content as needed and take full responsibility for the content of the publication.

Declaration of competing interest

The authors declare the following financial interests/personal relationships which may be considered as potential competing interests: Babica, Pavel reports financial support was provided by Horizon 2020 - grant agreement No. 825712 - OBERON. Babica, Pavel reports financial support was provided by Horizon 2020 - grant agreement No. 857560 - CETOCOEN Excellence. Babica, Pavel reports financial support was provided by Ministry of Education Youth and Sports of the Czech Republic - project LM2023069. Grosso, Marina reports financial support was provided by Masaryk University Faculty of Science - Internal Grant Agency. If there are other authors, they declare that they have no known competing financial interests or personal relationships that could have appeared to influence the work reported in this paper.

Acknowledgement

This work was supported from the European Union's Horizon 2020 research and innovation programme under grant agreement No. 825712 - OBERON and under grant agreement No. 857560 - CETOCOEN Excellence. This publication reflects only the author's view and the European Commission is not responsible for any use that may be made of the information it contains. M.G. was supported by the Internal Grant Agency project MUNI/IGA/1194/2021. Authors thank the RECETOX Research Infrastructure (No. LM2023069) financed by the Ministry of Education, Youth and Sports for supportive background. The graphical abstract was created using Biorender.com.

Appendix A. Supplementary data

Supplementary data to this article can be found online at https://doi.org/10.1016/j.fct.2025.115241.

Data availability

Data will be made available on request.

References

Al-Abdulla, R., Ferrero, H., Boronat-Belda, T., Soriano, S., Quesada, I., Alonso-Magdalena, P., 2023. Exploring the effects of metabolism-disrupting chemicals on pancreatic α-cell viability, gene expression and function: a screening testing approach. Int. J. Mol. Sci. 24, 1044. https://doi.org/10.3390/ijms24021044.

Al-Abdulla, R., Ferrero, H., Soriano, S., Boronat-Belda, T., Alonso-Magdalena, P., 2022. Screening of relevant metabolism-disrupting chemicals on pancreatic β-cells: evaluation of murine and human in vitro models. Int. J. Mol. Sci. 23, 4182. https://doi.org/10.3390/ijms23084182.

An, J., Jiang, J., Tang, W., Zhong, Y., Ren, G., Shang, Y., Yu, Z., 2023. Lipid metabolic disturbance induced by triphenyl phosphate and hydroxy metabolite in HepG2 cells. Ecotoxicol. Environ. Saf. 262, 115160. https://doi.org/10.1016/j.ecoenv.2023.115160.

Angrish, M.M., Kaiser, J.P., McQueen, C.A., Chorley, B.N., 2016. Tipping the balance: hepatotoxicity and the 4 apical key events of hepatic steatosis. Toxicol. Sci. 150, 261–268. https://doi.org/10.1093/toxsci/kfw018.

Arzumanian, V.A., Kiseleva, O.I., Poverennaya, E.V., 2021. The curious case of the HepG2 cell line: 40 years of expertise. Int. J. Mol. Sci. 22, 13135. https://doi.org/10.3390/ijms222313135.

Audouze, K., Sarigiannis, D., Alonso-Magdalena, P., Brochot, C., Casas, M., Vrijheid, M., Babin, P.J., Karakitsios, S., Coumoul, X., Barouki, R., 2020. Integrative strategy of testing systems for identification of endocrine disruptors inducing metabolic disorders—an introduction to the OBERON project. Int. J. Mol. Sci. 21, 2988. https://doi.org/10.3390/ijms21082988.

Bereketoglu, C., Häggblom, I., Turanlı, B., Pradhan, A., 2024. Comparative analysis of diisononyl phthalate and di(isononyl)cyclohexane-1,2 dicarboxylate plasticizers in regulation of lipid metabolism in 3T3-L1 cells. Environ. Toxicol. 39, 1245–1257. https://doi.org/10.1002/tox.24010.

Bernal, K., Touma, C., Erradhouani, C., Boronat-Belda, T., Gaillard, L., Al Kassir, S., Le Mentec, H., Martin-Chouly, C., Podechard, N., Lagadic-Gossmann, D., Langouet, S., Brion, F., Knoll-Gellida, A., Babin, P.J., Sovadinova, I., Babica, P., Andreau, K., Barouki, R., Vondracek, J., Alonso-Magdalena, P., Blanc, E., Kim, M.J., Coumoul, X., 2022. Combinatorial pathway disruption is a powerful approach to delineate metabolic impacts of endocrine disruptors. FEBS Lett. 596, 3107–3123. https://doi.org/10.1002/1873-3468.14465.

Bernal, K., Touma, C., Le-Grand, B., Rose, S., Degerli, S., Genêt, V., Lagadic-Gossmann, D., Coumoul, X., Martin-Chouly, C., Langouët, S., Blanc, E.B., 2024. Assessment of endocrine disruptor impacts on lipid metabolism in a fatty acid-supplemented HepaRG human hepatic cell line. Chemosphere 349, 140883. https://doi.org/10.1016/j.chemosphere.2023.140883.

Bonnet, L., Alexandersson, I., Baboota, R.K., Kroon, T., Oscarsson, J., Smith, U., Boucher, J., 2022. Cellular senescence in hepatocytes contributes to metabolic disturbances in NASH. Front. Endocrinol. 13, 957616. https://doi.org/10.3389/fendo.2022.957616.

Bucher, S., Jalili, P., Le Guillou, D., Begriche, K., Rondel, K., Martinais, S., Zalko, D., Corlu, A., Robin, M.-A., Fromenty, B., 2017. Bisphenol a induces steatosis in HepaRG cells using a model of perinatal exposure. Environ. Toxicol. 32, 1024–1036. https://doi.org/10.1002/tox.22301.

Campos-Espinosa, A., Guzmán, C., 2021. A model of experimental steatosis in vitro: hepatocyte cell culture in lipid overload-conditioned medium. JoVE 171, e62543. https://doi.org/10.3791/62543.

Cano, R., Pérez, J., Dávila, L., Ortega, Á., Gómez, Y., Valero-Cedeño, N., Parra, H., Manzano, A., Véliz Castro, T., Albornoz, M., Cano, G., Rojas-Quintero, J., Chacín, M., Bermúdez, V., 2021. Role of endocrine-disrupting chemicals in the pathogenesis of non-alcoholic fatty liver disease: a comprehensive review. Int. J. Mol. Sci. 22, 4807. https://doi.org/10.3390/ijms22094807.

Chen, Y., Wang, Y., Cui, Z., Liu, W., Liu, B., Zeng, Q., Zhao, X., Dou, J., Cao, J., 2023. Endocrine disrupting chemicals: a promoter of non-alcoholic fatty liver disease. Front. Public Health 11, 1154837. https://doi.org/10.3389/fpubh.2023.1154837.

Cui, H., Chang, Y., Cao, J., Jiang, X., Li, M., 2022. Liver immune and lipid metabolism disorders in mice induced by triphenyl phosphate with or without high fructose and high fat diet. Chemosphere 308, 136543. https://doi.org/10.1016/j.chemosphere.2022.136543.

Dallio, M., Masarone, M., Errico, S., Gravina, A.G., Nicolucci, C., Di Sarno, R., Gionti, L., Tuccillo, C., Persico, M., Stiuso, P., Diano, N., Loguercio, C., Federico, A., 2018. Role of bisphenol A as environmental factor in the promotion of non-alcoholic fatty liver disease: in vitro and clinical study. Aliment. Pharmacol. Ther. 47, 826–837. https://doi.org/10.1111/apt.14499.

Donato, M.T., Gallego-Ferrer, G., Tolosa, L., 2022. In vitro models for studying chronic drug-induced liver injury. Int. J. Mol. Sci. 23, 11428. https://doi.org/10.3390/ijms231911428.

Donato, M.T., Goméz-Lechón, M.J., 2012. Drug-induced liver steatosis and phospholipidosis: cell-based assays for early screening of drug candidates. Curr. Drug Metab. 13, 1160–1173. https://doi.org/10.2174/138920012802850001.

Donato, M.T., Tolosa, L., Jiménez, N., Castell, J.V., Gómez-Lechón, M.J., 2012. High-content imaging technology for the evaluation of drug-induced steatosis using a multiparametric cell-based assay. J. Biomol. Screen. 17, 394–400. https://doi.org/10.1177/1087057111427586.

Dong, Y., Cai, D., Liu, C., Zhao, S., Wang, L., 2023. Combined cytotoxicity of phthalate esters on HepG2 cells: a comprehensive analysis of transcriptomics and metabolomics. Food Chem. Toxicol. 180, 114034. https://doi.org/10.1016/j.fct.2023.114034.

Escher, S.E., Aguayo-Orozco, A., Benfenati, E., Bitsch, A., Braunbeck, T., Brotzmann, K., Bois, F., van der Burg, B., Castel, J., Exner, T., Gadaleta, D., Gardner, I., Goldmann, D., Hatley, O., Golbamaki, N., Graepel, R., Jennings, P., Limonciel, A., Long, A., Maclennan, R., Mombelli, E., Norinder, U., Jain, S., Capinha, L.S., Taboureau, O.T., Tolosa, L., Vrijenhoek, N.G., van Vugt-Lussenburg, B.M.A., Walker, P., van de Water, B., Wehr, M., White, A., Zdrazil, B., Fisher, C., 2022. Integrate mechanistic evidence from new approach methodologies (NAMs) into a read-across assessment to characterise trends in shared mode of action. Toxicol. Vitro 79, 105269. https://doi.org/10.1016/j.tiv.2021.105269.

Ferreira Azevedo, L., Masiero, M.M., Cherkaoui, S., Hornos Carneiro, M.F., Barbosa Jr, F., Zamboni, N., 2022. The alternative analog plasticizer BPS displays similar phenotypic and metabolomic responses to BPA in HepG2 and INS-1E cells. Food Chem. Toxicol. 167, 113266. https://doi.org/10.1016/j.fct.2022.113266.

Fragki, S., Dirven, H., Fletcher, T., Grasl-Kraupp, B., Bjerve Gützkow, K., Hoogenboom, R., Kersten, S., Lindeman, B., Louisse, J., Peijnenburg, A., Piersma, A. H., Princen, H.M.G., Uhl, M., Westerhout, J., Zeilmaker, M.J., Luijten, M., 2021. Systemic PFOS and PFOA exposure and disturbed lipid homeostasis in humans: what do we know and what not? Crit. Rev. Toxicol. 51, 141–164. https://doi.org/10.1080/10408444.2021.1888073.

Franco, M.E., Fernandez-Luna, M.T., Ramirez, A.J., Lavado, R., 2020. Metabolomic-based assessment reveals dysregulation of lipid profiles in human liver cells exposed to environmental obesogens. Toxicol. Appl. Pharmacol. 398, 115009. https://doi.org/10.1016/j.taap.2020.115009.

Fritsche, K., Ziková-Kloas, A., Marx-Stoelting, P., Braeuning, A., 2023. Metabolism-disrupting chemicals affecting the liver: screening, testing, and molecular pathway identification. Int. J. Mol. Sci. 24, 2686. https://doi.org/10.3390/ijms24032686.

Gómez-Lechón, M.J., Donato, M.T., Martínez-Romero, A., Jiménez, N., Castell, J.V., O'Connor, J.-E., 2007. A human hepatocellular in vitro model to investigate steatosis. Chem. Biol. Interact. 165, 106–116. https://doi.org/10.1016/j.cbi.2006.11.004.

Grünig, D., Duthaler, U., Krähenbühl, S., 2018. Effect of toxicants on fatty acid metabolism in HepG2 cells. Front. Pharmacol. 9, 257. https://doi.org/10.3389/fphar.2018.00257.

Hao, Z., Zhang, Z., Lu, D., Ding, B., Shu, L., Zhang, Q., Wang, C., 2019. Organophosphorus flame retardants impair intracellular lipid metabolic function in human hepatocellular cells. Chem. Res. Toxicol. 32, 1250–1258. https://doi.org/10.1021/acs.chemrestox.9b00058.

He, W., Guo, W., Qian, Y., Zhang, S., Ren, D., Liu, S., 2015. Synergistic hepatotoxicity by cadmium and chlorpyrifos: disordered hepatic lipid homeostasis. Mol. Med. Rep. 12, 303–308. https://doi.org/10.3892/mmr.2015.3381.
Heindel, J.J., Blumberg, B., Cave, M., Machtinger, R., Mantovani, A., Mendez, M.A., Nadal, A., Palanza, P., Panzica, G., Sargis, R., Vandenberg, L.N., vom Saal, F., 2017. Metabolism disrupting chemicals and metabolic disorders. Reprod. Toxicol. 68, 3–33. https://doi.org/10.1016/j.reprotox.2016.10.001.
Heindel, J.J., Howard, S., Agay-Shay, K., Arrebola, J.P., Audouze, K., Babin, P.J., Barouki, R., Bansal, A., Blanc, E., Cave, M.C., Chatterjee, S., Chevalier, N., Choudhury, M., Collier, D., Connolly, L., Coumoul, X., Garruti, G., Gilbertson, M., Hoepner, L.A., Holloway, A.C., Howell, G., Kassotis, C.D., Kay, M.K., Kim, M.J., Lagadic-Gossmann, D., Langouet, S., Legrand, A., Li, Z., Le Mentec, H., Lind, L., Monica Lind, P., Lustig, R.H., Martin-Chouly, C., Munic Kos, V., Podechard, N., Roepke, T.A., Sargis, R.M., Starling, A., Tomlinson, C.R., Touma, C., Vondracek, J., Vom Saal, F., Blumberg, B., 2022. Obesity II: establishing causal links between chemical exposures and obesity. Biochem. Pharmacol. 199, 115015. https://doi.org/10.1016/j.bcp.2022.115015.
Héliès-Toussaint, C., Peyre, L., Costanzo, C., Chagnon, M.-C., Rahmani, R., 2014. Is bisphenol S a safe substitute for bisphenol A in terms of metabolic function? An in vitro study. Toxicol. Appl. Pharmacol. 280, 224–235. https://doi.org/10.1016/j.taap.2014.07.025.
Huc, L., Lemarié, A., Guéraud, F., Héliès-Toussaint, C., 2012. Low concentrations of bisphenol A induce lipid accumulation mediated by the production of reactive oxygen species in the mitochondria of HepG2 cells. Toxicol. Vitro 26, 709–717. https://doi.org/10.1016/j.tiv.2012.03.017.
Ipsen, D.H., Lykkesfeldt, J., Tveden-Nyborg, P., 2018. Molecular mechanisms of hepatic lipid accumulation in non-alcoholic fatty liver disease. Cell. Mol. Life Sci. 75, 3313–3327. https://doi.org/10.1007/s00018-018-2860-6.
Ji, G., Xu, C., Sun, H., Liu, Q., Hu, H., Gu, A., Jiang, Z.-Y., 2016. Organochloride pesticides induced hepatic ABCG5/G8 expression and lipogenesis in Chinese patients with gallstone disease. Oncotarget 7, 33689–33702. https://doi.org/10.18632/oncotarget.9399.
Kong, A., Zhang, Y., Ning, B., Li, K., Ren, Z., Dai, S., Chen, D., Zhou, Y., Gu, J., Shi, H., 2021. Cadmium induces triglyceride levels via microsomal triglyceride transfer protein (MTTP) accumulation caused by lysosomal deacidification regulated by endoplasmic reticulum (ER) Ca2+ homeostasis. Chem. Biol. Interact. 348, 109649. https://doi.org/10.1016/j.cbi.2021.109649.
Kõressaar, T., Lepamets, M., Kaplinski, L., Raime, K., Andreson, R., Remm, M., 2018. Primer3_masker: integrating masking of template sequence with primer design software. Bioinformatics 34, 1937–1938. https://doi.org/10.1093/bioinformatics/bty036.
Kowalczyk, M., Piwowarski, J.P., Wardaszka, A., Średnicka, P., Wójcicki, M., Juszczuk-Kubiak, E., 2023. Application of in vitro models for studying the mechanisms underlying the obesogenic action of endocrine-disrupting chemicals (EDCs) as food contaminants—a review. Int. J. Mol. Sci. 24, 1083. https://doi.org/10.3390/ijms24021083.
Kubickova, B., Jacobs, M.N., 2023. Development of a reference and proficiency chemical list for human steatosis endpoints in vitro. Front. Endocrinol. 14, 1126880. https://doi.org/10.3389/fendo.2023.1126880.
Küblbeck, J., Vuorio, T., Niskanen, J., Fortino, V., Braeuning, A., Abass, K., Rautio, A., Hakkola, J., Honkakoski, P., Levonen, A.-L., 2020. The EDCMET project: metabolic effects of endocrine disruptors. Int. J. Mol. Sci. 21, 3021. https://doi.org/10.3390/ijms21083021.
Kucera, J., Chalupova, Z., Wabitsch, M., Bienertova-Vasku, J., 2024. Endocrine disruption of adipose physiology: screening in SGBS cells. J. Appl. Toxicol. 44, 1784–1792. https://doi.org/10.1002/jat.4679.
Le Mentec, H., Monniez, E., Legrand, A., Monvoisin, C., Lagadic-Gossmann, D., Podechard, N., 2023. A new in vivo zebrafish bioassay evaluating liver steatosis identifies DDE as a steatogenic endocrine disruptor, partly through SCD1 regulation. Int. J. Mol. Sci. 24, 3942. https://doi.org/10.3390/ijms24043942.
Legler, J., Zalko, D., Jourdan, F., Jacobs, M., Fromenty, B., Balaguer, P., Bourguet, W., Munic Kos, V., Nadal, A., Beausoleil, C., Cristobal, S., Remy, S., Ermler, S., Margiotta-Casaluci, L., Griffin, J.L., Blumberg, B., Chesné, C., Hoffmann, S., Andersson, P.L., Kamstra, J.H., 2020. The GOLIATH project: towards an internationally harmonised approach for testing metabolism disrupting compounds. Int. J. Mol. Sci. 21, 3480. https://doi.org/10.3390/ijms21103480.
Lichtenstein, D., Luckert, C., Alarcan, J., De Sousa, G., Gioutlakis, M., Katsanou, E.S., Konstantinidou, P., Machera, K., Milani, E.S., Peijnenburg, A., Rahmani, R., Rijkers, D., Spyropoulou, A., Stamou, M., Stoopen, G., Sturla, S.J., Wollscheid, B., Zucchini-Pascal, N., Braeuning, A., Lampen, A., 2020. An adverse outcome pathway-based approach to assess steatotic mixture effects of hepatotoxic pesticides in vitro. Food Chem. Toxicol. 139, 111283. https://doi.org/10.1016/j.fct.2020.111283.
Lin, Y., Ding, D., Huang, Q., Liu, Q., Lu, H., Lu, Y., Chi, Y., Sun, X., Ye, G., Zhu, H., Wei, J., Dong, S., 2017. Downregulation of miR-192 causes hepatic steatosis and lipid accumulation by inducing SREBF1: novel mechanism for bisphenol A-triggered non-alcoholic fatty liver disease. Biochim. Biophys. Acta Mol. Cell Biol. Lipids 1862, 869–882. https://doi.org/10.1016/j.bbalip.2017.05.001.
Ling, J., Hua, L., Qin, Y., Gu, T., Jiang, S., Zhao, J., 2023. Perfluorooctane sulfonate promotes hepatic lipid accumulation and steatosis in high-fat diet mice through AMP-activated protein kinase/acetyl-CoA carboxylase (AMPK/ACC) pathway. J. Appl. Toxicol. 43, 312–322. https://doi.org/10.1002/jat.4383.
Liu, Q., Shao, W., Weng, Z., Zhang, X., Ding, G., Xu, C., Xu, J., Jiang, Z., Gu, A., 2020. In vitro evaluation of the hepatic lipid accumulation of bisphenol analogs: a high-content screening assay. Toxicol. Vitro 68, 104959. https://doi.org/10.1016/j.tiv.2020.104959.
Liu, Q., Wang, Q., Xu, C., Shao, W., Zhang, C., Liu, H., Jiang, Z., Gu, A., 2017. Organochloride pesticides impaired mitochondrial function in hepatocytes and aggravated disorders of fatty acid metabolism. Sci. Rep. 7, 46339. https://doi.org/10.1038/srep46339.
Liu, X., Hu, M., Ye, C., Liao, L., Ding, C., Sun, L., Liang, J., Chen, Y., 2022. Isosilybin regulates lipogenesis and fatty acid oxidation via the AMPK/SREBP-1c/PPARα pathway. Chem. Biol. Interact. 368, 110250. https://doi.org/10.1016/j.cbi.2022.110250.
Livak, K.J., Schmittgen, T.D., 2001. Analysis of relative gene expression data using real-time quantitative PCR and the 2(-Delta Delta C(T)) Method. Methods 25, 402–408. https://doi.org/10.1006/meth.2001.1262.
Louisse, J., Rijkers, D., Stoopen, G., Janssen, A., Staats, M., Hoogenboom, R., Kersten, S., Peijnenburg, A., 2020. Perfluorooctanoic acid (PFOA), perfluorooctane sulfonic acid (PFOS), and perfluorononanoic acid (PFNA) increase triglyceride levels and decrease cholesterogenic gene expression in human HepaRG liver cells. Arch. Toxicol. 94, 3137–3155. https://doi.org/10.1007/s00204-020-02808-0.
Migni, A., Mancuso, F., Baroni, T., Di Sante, G., Rende, M., Galli, F., Bartolini, D., 2023. Melatonin as a repairing agent in cadmium- and free fatty acid-induced lipotoxicity. Biomolecules 13, 1758. https://doi.org/10.3390/biom13121758.
Miquilena-Colina, M.E., Lima-Cabello, E., Sanchez-Campos, S., Garcia-Mediavilla, M.V., Fernandez-Bermejo, M., Lozano-Rodriguez, T., Vargas-Castrillon, J., Buque, X., Ochoa, B., Aspichueta, P., Gonzalez-Gallego, J., Garcia-Monzon, C., 2011. Hepatic fatty acid translocase CD36 upregulation is associated with insulin resistance, hyperinsulinaemia and increased steatosis in non-alcoholic steatohepatitis and chronic hepatitis C. Gut 60, 1394–1402. https://doi.org/10.1136/gut.2010.222844.
Mosca, A., Manco, M., Braghini, M.R., Cianfarani, S., Maggiore, G., Alisi, A., Vania, A., 2024. Environment, endocrine disruptors, and fatty liver disease associated with metabolic dysfunction (MASLD). Metabolites 14, 71. https://doi.org/10.3390/metabo14010071.
Negi, C.K., Bajard, L., Kohoutek, J., Blaha, L., 2021. An adverse outcome pathway based in vitro characterization of novel flame retardants-induced hepatic steatosis. Environ. Pollut. 289, 117855. https://doi.org/10.1016/j.envpol.2021.117855.
Niture, S., Gadi, S., Lin, M., Qi, Q., Niture, S.S., Moore, J.T., Bodnar, W., Fernando, R.A., Levine, K.E., Kumar, D., 2023. Cadmium modulates steatosis, fibrosis, and oncogenic signaling in liver cancer cells by activating notch and AKT/mTOR pathways. Environ. Toxicol. 38, 783–797. https://doi.org/10.1002/tox.23731.
Ozyurt, B., Ozkemahli, G., Yirun, A., Ozyurt, A.B., Bacanli, M., Basaran, N., Kocer-Gumusel, B., Erkekoglu, P., 2023. Comparative evaluation of the effects of bisphenol derivatives on oxidative stress parameters in HepG2 cells. Drug Chem. Toxicol. 46, 314–322. https://doi.org/10.1080/01480545.2022.2028823.
Park, S., Choi, Y.-J., Lee, B.-H., 2012. In vitro validation of drug-induced phospholipidosis. J. Toxicol. Sci. 37, 261–267. https://doi.org/10.2131/jts.37.261.
Peyre, L., Rouimi, P., De Sousa, G., Héliès-Toussaint, C., Carré, B., Barcellini, S., Chagnon, M.-C., Rahmani, R., 2014. Comparative study of bisphenol A and its analogue bisphenol S on human hepatic cells: a focus on their potential involvement in nonalcoholic fatty liver disease. Food Chem. Toxicol. 70, 9–18. https://doi.org/10.1016/j.fct.2014.04.011.
Qi, Q., Niture, S., Gadi, S., Arthur, E., Moore, J., Levine, K.E., Kumar, D., 2023. Per- and polyfluoroalkyl substances activate UPR pathway, induce steatosis and fibrosis in liver cells. Environ. Toxicol. 38, 225–242. https://doi.org/10.1002/tox.23680.
Qi, W., Clark, J.M., Timme-Laragy, A.R., Park, Y., 2020. Perfluorobutanesulfonic acid (PFBS) induces fat accumulation in HepG2 human hepatoma. Toxicol. Environ. Chem. 102, 585–606. https://doi.org/10.1080/02772248.2020.1808894.
Rada, P., González-Rodríguez, Á., García-Monzón, C., Valverde, Á.M., 2020. Understanding lipotoxicity in NAFLD pathogenesis: is CD36 a key driver? Cell Death Dis. 11, 802. https://doi.org/10.1038/s41419-020-03003-w.
Raška, J., Čtveráčková, L., Dydowiczová, A., Sovadinová, I., Bláha, L., Babica, P., 2018. Tumor-promoting cyanotoxin microcystin-LR does not induce procarcinogenic events in adult human liver stem cells. Toxicol. Appl. Pharmacol. 345, 103–113. https://doi.org/10.1016/j.taap.2018.03.011.
Ren, Y., Shi, X., Mu, J., Liu, S., Qian, X., Pei, W., Ni, S., Zhang, Zhengduo, Li, L., Zhang, Zhan, 2024. Chronic exposure to parabens promotes non-alcoholic fatty liver disease in association with the changes of the gut microbiota and lipid metabolism. Food Funct. 15, 1562–1574. https://doi.org/10.1039/D3FO04347A.
Rinella, M.E., Lazarus, J.V., Ratziu, V., Francque, S.M., Sanyal, A.J., Kanwal, F., Romero, D., Abdelmalek, M.F., Anstee, Q.M., Arab, J.P., Arrese, M., Bataller, R., Beuers, U., Boursier, J., Bugianesi, E., Byrne, C.D., Castro Narro, G.E., Chowdhury, A., Cortez-Pinto, H., Cryer, D.R., Cusi, K., El-Kassas, M., Klein, S., Eskridge, W., Fan, J., Gawrieh, S., Guy, C.D., Harrison, S.A., Kim, S.U., Koot, B.G., Korenjak, M., Kowdley, K.V., Lacaille, F., Loomba, R., Mitchell-Thain, R., Morgan, T. R., Powell, E.E., Roden, M., Romero-Gómez, M., Silva, M., Singh, S.P., Sookoian, S. C., Spearman, C.W., Tiniakos, D., Valenti, L., Vos, M.B., Wong, V.W.-S., Xanthakos, S., Yilmaz, Y., Younossi, Z., Hobbs, A., Villota-Rivas, M., Newsome, P.N., 2023. A multisociety Delphi consensus statement on new fatty liver disease nomenclature. J. Hepatol. 79, 1542–1556. https://doi.org/10.1016/j.jhep.2023.06.003.
Rogue, A., Anthérieu, S., Vluggens, A., Umbdenstock, T., Claude, N., De La Moureyre-Spire, C., Weaver, R.J., Guillouzo, A., 2014. PPAR agonists reduce steatosis in oleic acid-overloaded HepaRG cells. Toxicol. Appl. Pharmacol. 276, 73–81. https://doi.org/10.1016/j.taap.2014.02.001.
Saad, N., Bereketoglu, C., Pradhan, A., 2021. Di(isononyl) cyclohexane-1,2-dicarboxylate (DINCH) alters transcriptional profiles, lipid metabolism and behavior in zebrafish larvae. Heliyon 7, e07951. https://doi.org/10.1016/j.heliyon.2021.e07951.
Sadrabadi, F., Alarcan, J., Sprenger, H., Braeuning, A., Buhrke, T., 2024. Impact of perfluoroalkyl substances (PFAS) and PFAS mixtures on lipid metabolism in

differentiated HepaRG cells as a model for human hepatocytes. Arch. Toxicol. 98, 507–524. https://doi.org/10.1007/s00204-023-03649-3.
Schaffert, A., Karkossa, I., Ueberham, E., Schlichting, R., Walter, K., Arnold, J., Blüher, M., Heiker, J.T., Lehmann, J., Wabitsch, M., Escher, B.I., Von Bergen, M., Schubert, K., 2022. Di-(2-ethylhexyl) phthalate substitutes accelerate human adipogenesis through PPARγ activation and cause oxidative stress and impaired metabolic homeostasis in mature adipocytes. Environ. Int. 164, 107279. https://doi.org/10.1016/j.envint.2022.107279.
Sheedfar, F., Sung, M.M., Aparicio-Vergara, M., Kloosterhuis, N.J., Miquilena-Colina, M. E., Vargas-Castrillón, J., Febbraio, M., Jacobs, R.L., De Bruin, A., Vinciguerra, M., García-Monzón, C., Hofker, M.H., Dyck, J.R., Koonen, D.P., 2014. Increased hepatic CD36 expression with age is associated with enhanced susceptibility to nonalcoholic fatty liver disease. Aging 6, 281–295. https://doi.org/10.18632/aging.100652.
Shimpi, P.C., More, V.R., Paranjpe, M., Donepudi, A.C., Goodrich, J.M., Dolinoy, D.C., Rubin, B., Slitt, A.L., 2017. Hepatic lipid accumulation and Nrf2 expression following perinatal and peripubertal exposure to bisphenol A in a mouse model of nonalcoholic liver disease. Environ. Health Perspect. 125, 087005. https://doi.org/10.1289/EHP664.
Shree Harini, K., Ezhilarasan, D., 2023. Wnt/beta-catenin signaling and its modulators in nonalcoholic fatty liver diseases. Hepatobiliary Pancreat. Dis. Int. 22, 333–345. https://doi.org/10.1016/j.hbpd.2022.10.003.
Song, Y., Zhang, Cui, Lei, H., Qin, M., Chen, G., Wu, F., Chen, C., Cao, Z., Zhang, Ce, Wu, M., Chen, X., Zhang, L., 2022. Characterization of triclosan-induced hepatotoxicity and triclocarban-triggered enterotoxicity in mice by multiple omics screening. Sci. Total Environ. 838, 156570. https://doi.org/10.1016/j.scitotenv.2022.156570.
Stossi, F., Dandekar, R.D., Johnson, H., Lavere, P., Foulds, C.E., Mancini, M.G., Mancini, M.A., 2019. Tributyltin chloride (TBT) induces RXRA down-regulation and lipid accumulation in human liver cells. PLoS One 14, e0224405. https://doi.org/10.1371/journal.pone.0224405.
Teixeira, F.S., Pimentel, L.L., Pintado, M.E., Rodríguez-Alcalá, L.M., 2023. Impaired hepatic lipid metabolism and biomarkers in fatty liver disease. Biochimie 215, 69–74. https://doi.org/10.1016/j.biochi.2023.09.020.
Tolosa, L., Gómez-Lechón, M.J., Jiménez, N., Hervás, D., Jover, R., Donato, M.T., 2016. Advantageous use of HepaRG cells for the screening and mechanistic study of drug-induced steatosis. Toxicol. Appl. Pharmacol. 302, 1–9. https://doi.org/10.1016/j.taap.2016.04.007.
Tolosa, L., Pinto, S., Donato, M.T., Lahoz, A., Castell, J.V., O'Connor, J.E., Gómez-Lechón, M.J., 2012. Development of a multiparametric cell-based protocol to screen and classify the hepatotoxicity potential of drugs. Toxicol. Sci. 127, 187–198. https://doi.org/10.1093/toxsci/kfs083.
Vandenberg, L.N., Colborn, T., Hayes, T.B., Heindel, J.J., Jacobs, D.R., Lee, D.-H., Shioda, T., Soto, A.M., Vom Saal, F.S., Welshons, W.V., Zoeller, R.T., Myers, J.P., 2012. Hormones and endocrine-disrupting chemicals: low-dose effects and nonmonotonic dose responses. Endocr. Rev. 33, 378–455. https://doi.org/10.1210/er.2011-1050.
Vandesompele, J., De Preter, K., Pattyn, F., Poppe, B., Van Roy, N., De Paepe, A., Speleman, F., 2002. Accurate normalization of real-time quantitative RT-PCR data by geometric averaging of multiple internal control genes. Genome Biol. 3. https://doi.org/10.1186/gb-2002-3-7-research0034 research0034.1.
Vanova, T., Raska, J., Babica, P., Sovadinova, I., Kunova Bosakova, M., Dvorak, P., Blaha, L., Rotrekl, V., 2019. Freshwater cyanotoxin cylindrospermopsin has detrimental stage-specific effects on hepatic differentiation from human embryonic stem cells. Toxicol. Sci. 168, 241–251. https://doi.org/10.1080/15287390701434877.
Vasconcelos, A.L., Silva, M.J., Louro, H., 2019. In vitro exposure to the next-generation plasticizer diisononyl cyclohexane-1,2-dicarboxylate (DINCH): cytotoxicity and genotoxicity assessment in human cells. J. Toxicol. Environ. Health, Part A 82, 526–536. https://doi.org/10.1080/15287394.2019.1634376.
Vilas-Boas, V., Gijbels, E., Leroy, K., Pieters, A., Baze, A., Parmentier, C., Vinken, M., 2021. Primary human hepatocyte spheroids as tools to study the hepatotoxic potential of non-pharmaceutical chemicals. Int. J. Mol. Sci. 22, 11005. https://doi.org/10.3390/ijms222011005.
Wang, D., Yan, S., Yan, J., Teng, M., Meng, Z., Li, R., Zhou, Z., Zhu, W., 2019. Effects of triphenyl phosphate exposure during fetal development on obesity and metabolic dysfunctions in adult mice: impaired lipid metabolism and intestinal dysbiosis. Environ. Pollut. 246, 630–638. https://doi.org/10.1016/j.envpol.2018.12.053.
Wang, J., Yu, P., Xie, X., Wu, L., Zhou, M., Huan, F., Jiang, L., Gao, R., 2021. Bisphenol F induces nonalcoholic fatty liver disease-like changes: involvement of lysosome disorder in lipid droplet deposition. Environ. Pollut. 271, 116304. https://doi.org/10.1016/j.envpol.2020.116304.
Wen, Y., Mirji, N., Irudayaraj, J., 2020. Epigenetic toxicity of PFOA and GenX in HepG2 cells and their role in lipid metabolism. Toxicol. Vitro 65, 104797. https://doi.org/10.1016/j.tiv.2020.104797.
Weng, Z., Xu, C., Zhang, X., Pang, L., Xu, J., Liu, Q., Zhang, L., Xu, S., Gu, A., 2020. Autophagy mediates perfluorooctanoic acid-induced lipid metabolism disorder and NLRP3 inflammasome activation in hepatocytes. Environ. Pollut. 267, 115655. https://doi.org/10.1016/j.envpol.2020.115655.
Xiang, D., Wang, Q., 2021. PXR-mediated organophorous flame retardant tricresyl phosphate effects on lipid homeostasis. Chemosphere 284, 131250. https://doi.org/10.1016/j.chemosphere.2021.131250.
Yang, S., Ooka, M., Margolis, R.J., Xia, M., 2023. Liver three-dimensional cellular models for high-throughput chemical testing. Cell Rep. Methods 3, 100432. https://doi.org/10.1016/j.crmeth.2023.100432.
Yu, D., Hales, B.F., Robaire, B., 2024. Organophosphate ester flame retardants and plasticizers affect the phenotype and function of HepG2 liver cells. Toxicol. Sci. 199, 261–275. https://doi.org/10.1093/toxsci/kfae034.
Yueh, M.-F., He, F., Chen, C., Vu, C., Tripathi, A., Knight, R., Karin, M., Chen, S., Tukey, R.H., 2020. Triclosan leads to dysregulation of the metabolic regulator FGF21 exacerbating high fat diet-induced nonalcoholic fatty liver disease. Proc. Natl. Acad. Sci. U.S.A. 117, 31259–31266. https://doi.org/10.1073/pnas.2017129117.
Zhang, H., Shao, X., Zhao, H., Li, X., Wei, J., Yang, C., Cai, Z., 2019. Integration of metabolomics and lipidomics reveals metabolic mechanisms of triclosan-induced toxicity in human hepatocytes. Environ. Sci. Technol. 53, 5406–5415. https://doi.org/10.1021/acs.est.8b07281.
Zhang, W., Li, J.-Y., Wei, X.-C., Wang, Q., Yang, J.-Y., Hou, H., Du, Z.-W., Wu, X.-A., 2021. Effects of dibutyl phthalate on lipid metabolism in liver and hepatocytes based on PPARα/SREBP-1c/FAS/GPAT/AMPK signal pathway. Food Chem. Toxicol. 149, 112029. https://doi.org/10.1016/j.fct.2021.112029.
Zhang, W., Shen, X.-Y., Zhang, W.-W., Chen, H., Xu, W.-P., Wei, W., 2017. The effects of di 2-ethyl hexyl phthalate (DEHP) on cellular lipid accumulation in HepG2 cells and its potential mechanisms in the molecular level. Toxicol. Mech. Methods 27, 245–252. https://doi.org/10.1080/15376516.2016.1273427.